



Constraints on Fluid Evolution at the Polymetallic Lustdust Porphyry-Skarn-Manto-Vein Prospect, North-Central British Columbia

By Kathryn P.E. Dunne¹, and Gerald. E. Ray²

KEYWORDS: *Fluid inclusions, Lustdust, porphyry, skarn, manto, vein, hydrothermal fluids, salinity, homogenization temperature, pressure, H₂O, NaCl, CaCl₂, CO₂, fluid immiscibility, Takla Silver Mine, high sulphidation veins, economic geology, exploration.*

INTRODUCTION

Alpha Gold Corp's Lustdust Cu-Mo-Au-Zn-Pb-Ag property lies approximately 210 km northwest of Prince George and 35 km northeast of Takla Lake in central British Columbia (Figure 1). It includes a skarn-manto-vein system related to an undeformed Mo-Cu-bearing porphyry body, the Glover Stock (Figure 2). A preliminary U-Pb zircon age of 51-52 Ma (Eocene) has been obtained on a dioritic phase of the porphyry (R. Friedman, personal communication, 2001; Ray *et al.* 2002, this volume). The stock intrudes a north-northwest trending belt of deformed oceanic metasedimentary and volcanic rocks which are part of the Carboniferous to Early Jurassic Cache Creek Terrane (Monger 1977, 1998; Paterson, 1977; Wheeler *et al.*, 1991; Gabrielse and Yorath, 1992; Schiarizza and MacIntyre, 1999; Schiarizza, 2000). The property lies less than 2 km west of the north-northwest trending Pinchi Fault which is a major dextral transform fault (Patterson, 1974; 1977). It separates the Cache Creek rocks from an intrusive suite immediately to the east belonging to the Quesnel Terrane (Gabriels and Yorath, 1992; Figure 1).

At Lustdust, mineralization is discontinuously traced for 2.5 km, from the porphyry-style mineralization in the north, to the quartz-sulphide-sulfosalt-bearing veins at the old Takla Silver Mine (Minfile 093N 008) in the south (Figure 2). Lustdust represents a classic mineralogically and chemically zoned, intrusion-related system (Evans, 1996; 1998; Megaw, 1999, 2000, 2001; Ray *et al.*, 2002, this volume). Proximal Cu-Mo porphyry style mineralization passes southwards into carbonate hosted Cu-Au (Zn) skarns and massive sphalerite-dominant mantos. The most southern expression of mineralization are massive sulphide-sulphosalt veins at the Takla Silver Mine; these veins, also known as the No. 1 Zone (Evans, 1996, 1998; Megaw 1999, 2000), are marked by Zn, Ag, Pb, Au, Hg, Sb and As enrichment (Ray *et al.*, 2002, this volume).

This paper presents the results of a fluid inclusion study of samples taken from the various styles mineralization at Lustdust. The sphalerite present in the skarns and mantos was too opaque for fluid inclusion work; instead, attempts were made to document fluid inclusion characteristics of garnets in the skarns, of igneous quartz phenocrysts in the Glover Stock, and of quartz from barren and mineralized veins in the porphyry, mantos and No 1 Zone veins. This work helped to evaluate changes in temperature and/or fluid composition throughout the system, examine evidence for fluid immiscibility, and estimate depths of emplacement of the intrusion and related mineralization. These data place constraints on fluid evolution at the Lustdust prospect.

GEOLOGIC SETTING

The Lustdust property is underlain by Cache Creek Group rocks, which comprise a steeply dipping, northerly striking package of deformed and weakly metamorphosed phyllites, cherts, mafic tuffs and volcanics, as well as thick (c. 500m) units of limestone. Microfossils, extracted from limestones hosting the Lustdust mineralization, are Mid to late Permian age (M.J. Orchard, personal communication, 2001; Ray *et al.*, 2002, this volume). These metasedimentary and metavolcanic rocks have a complex history of brittle-ductile deformation which was probably related to both the accretion of the Cache Creek Group onto the north American continent, and later recurrent dextral transcurrent movements along the Pinchi Fault Zone (Monger, 1977, 1998; Paterson, 1977; Gabrielse and Yorath, 1992).

The deformed supracrustal rocks are intruded by a north-northwest-trending swarm of felsic dikes and sills related to the small, post-tectonic Glover Stock (Figure 2). The elongate stock outcrops north and south of Canyon Creek and is surrounded by a narrow (< 300m) hornfelsic aureole. The stock is a multiphase intrusion ranging compositionally from mafic, amphibole-bearing diorite-monzodiorite to more felsic monzonite-quartz monzonite (Ray *et al.*, 2002, this volume). Analyses confirm the mafic phases are calcalkaline but the more felsic monzonitic suites have alkalic affinities; it is uncertain whether the latter chemical feature is primary or the result of hydrothermal overprinting by K-spar and sericite (Ray *et al.*, 2002, this volume). The stock hosts porphyry-style, Cu-Mo-bearing quartz veins and either it, or a related intrusive phase at depth, is believed to be genetically related to the adjacent skarn, manto and vein mineralization (Megaw, 2000, 2001).

¹ Consulting Geologist

² British Columbia Ministry of Energy and Mines

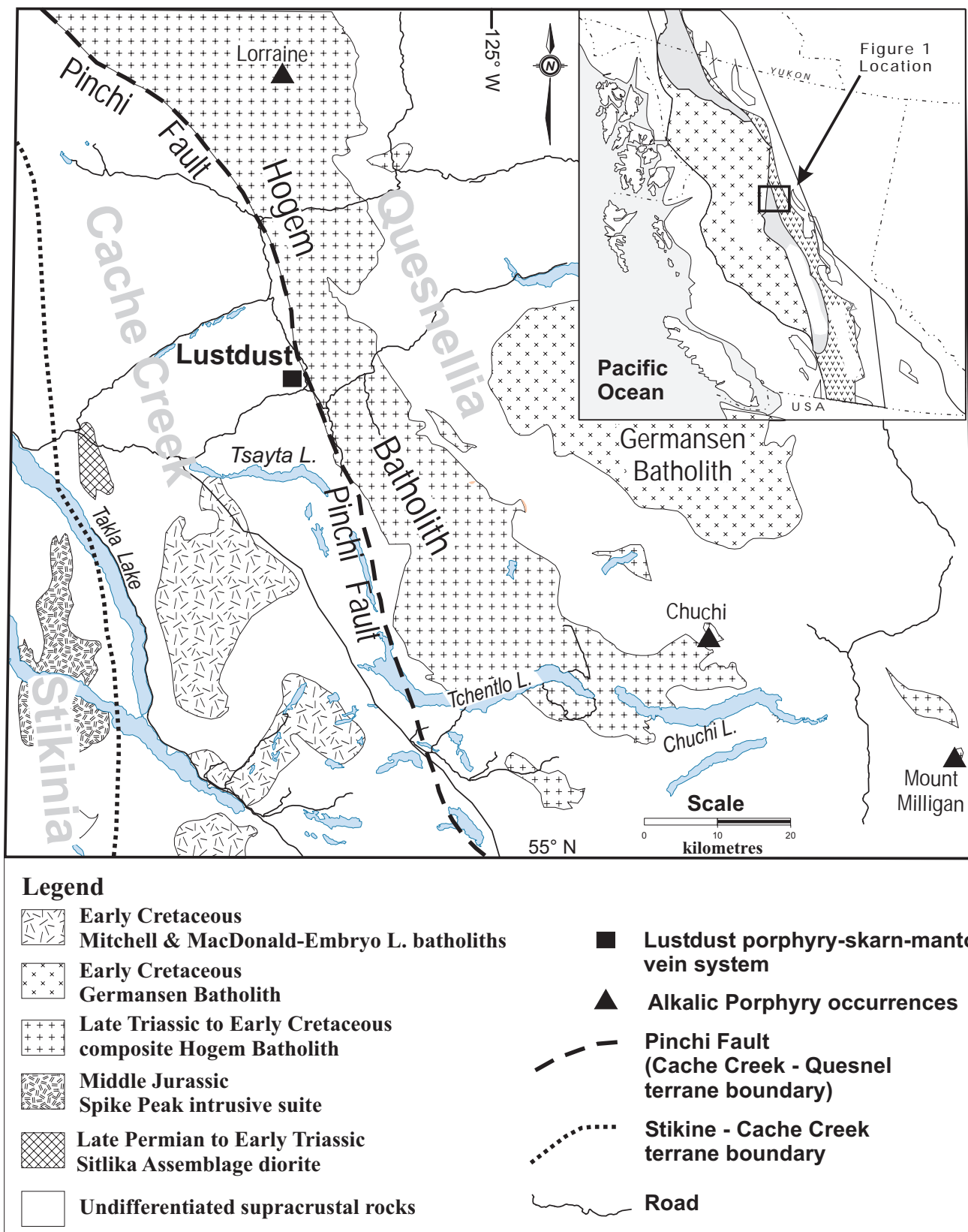


Figure 1. Takla Lake area showing the location of Lustdust property, the Pinchi Fault, the terrane boundaries and major intrusions. Geology after Wheeler *et al.* (1991) and The MapPlace, October, 2001.

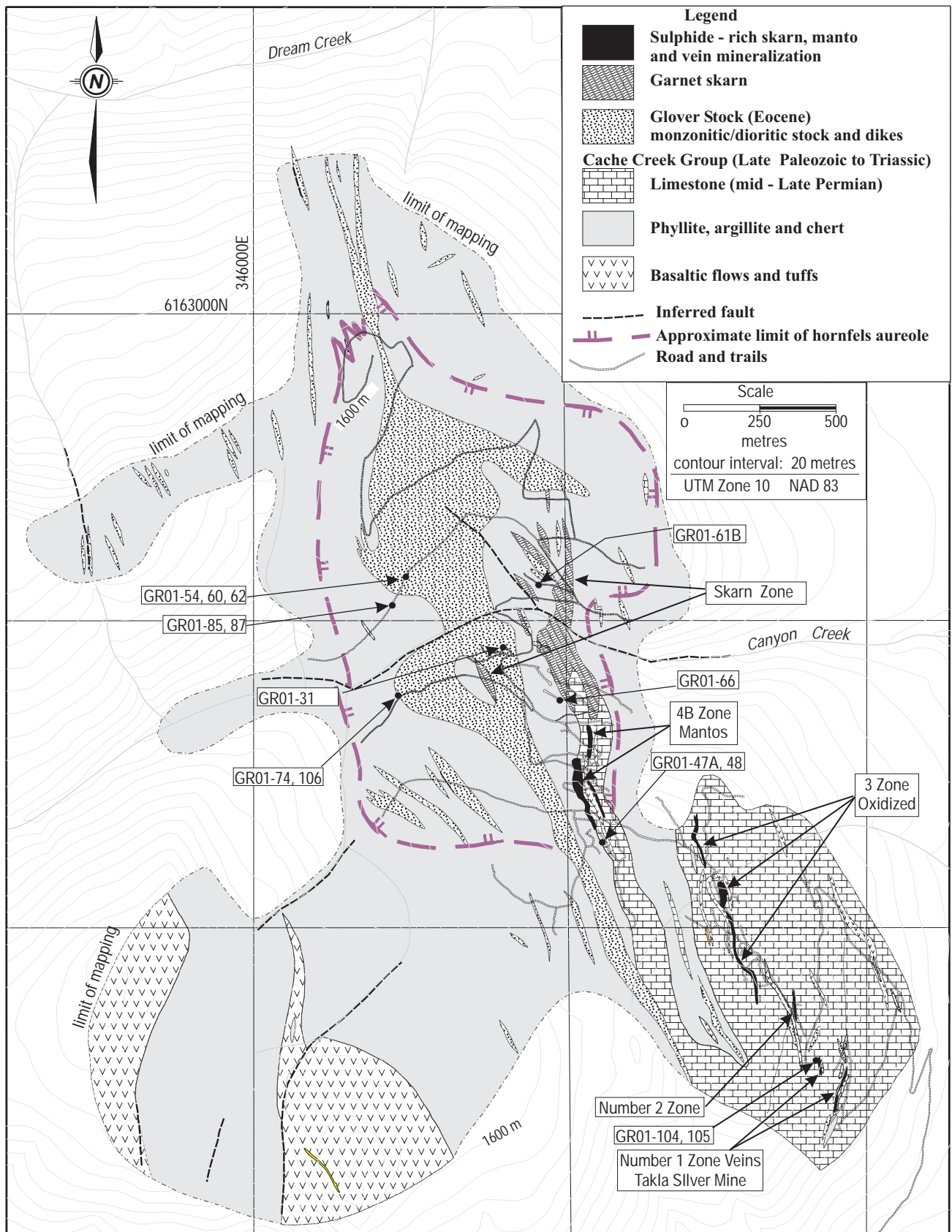


Figure 2. Geology of the Lustdust property showing location of the mineralized zones and samples collected for this study. Geology compiled from mapping by Evans (1996; 1998), Megaw (1999; 2000, 2001), and Ray *et al.* (2002, this volume).

The Lustdust mineralization extends discontinuously over a strike distance of 2.5 km (Figure 2). Samples were collected from the four main styles of mineralization named, from north to south, as follows (Table 1): the porphyry in the Glover Stock which lies north and south of Canyon Creek (Figure 2), the skarn zone, the sphalerite-rich mantos (4B Zone) and the No. 1 Zone veins which lie in the vicinity of the Takla Silver Mine (Figure 2). Megaw (2000, 2001) and Ray *et al.* (2002, this volume) describe details of the mineralization in each of these localities.

METHOD OF FLUID INCLUSION STUDY

Twenty-seven hand samples selected from outcrop and drillcore were collected for fluid inclusion, petrographic examination. They were selected to best represent the different styles of mineralization and alteration observed on the property. The samples included the following minerals which were of particular interest for this study (Table 1): (1) igneous quartz phenocrysts from the Glover Stock diorite and monzonite, (2) hydrothermal quartz from barren and mineralized Cu-Mo veins in the porphyry, (3) garnet and calcite crystals in the skarn, (4) quartz crystals in blebs in the massive 4B Zone sphalerite mantos, and (5) quartz and calcite from the quartz-sulphide-sulfosalt-bearing veins in the No. 1 Zone. Fluid inclusion shapes and sizes, spatial relationships among inclusions and minerals, and phases within inclusions were microscopically observed in doubly-polished thick sections. Based on this preliminary work, fifteen samples containing representative populations of inclusions from the different areas were selected for heating/freezing studies (Figure 2, Table 1).

Microthermometric data were obtained using a Fluid Inc. adapted USGS gas-flow heating-freezing stage housed at the Mineral Deposit Research Unit, Department of Earth and Ocean Sciences, The University of British Columbia. Calibration of the stage was achieved using commercial Syn Flic synthetic fluid inclusions and ice with the following accuracies: at $-56.6 \pm 0.2^\circ\text{C}$, $374.1 \pm 1^\circ\text{C}$ and $0.0 \pm 0.1^\circ\text{C}$. Fluid inclusion data were obtained by first freezing mineral chips and then observing CO_2 melting (if CO_2 present), first and final melting temperatures of ice, melting of salt-hydrates and gas-hydrates (clathrates), and where possible CO_2 homogenization (if CO_2 present) during heating. High temperature data (liquid-vapour homogenization and salt dissolution) were then collected from fluid inclusion assemblages in each mineral chip by incrementally heating above room temperature. Phase transitions in all inclusions were monitored during this heating run to avoid repeat heating and the resultant stretching of fluid inclusions.

Fluid inclusions were evaluated using the concept of fluid inclusion assemblages (FIA's). This ensures that the data was not biased by samples containing large numbers of fluid inclusions and helps to eliminate inconsistent data caused by changes in mass, volume or shape of inclusions after entrapment (*i.e.*, eliminate non-representative inclusions that are the result of diffusion, stretching, or necking-down processes). A fluid inclusion assemblage (FIA) is a petrographically-associated group of inclusions such as

those aligned along primary growth zones or secondary fracture planes. One representative data point, rather than several data points is used for each FIA.

RESULTS OF FLUID INCLUSION STUDY

The sphalerite crystals in the mantos were too opaque to determine their fluid inclusion characteristics. Instead, quartz and pale-yellow/green garnet were used for microthermometric analyses because of their optical clarity and high tensile strength; calcite was used in some samples for comparison. Fluid inclusions in quartz and calcite minerals ranged in maximum diameter from less than 1 micron to 30 microns; most measured fluid inclusions averaged 10 to 15 microns. Those in garnet from the skarn were significantly larger, averaging from 20 to 65 microns, and decrepitated inclusions over 100 microns were also observed.

FLUID INCLUSION POPULATIONS

Fluid inclusions were divided into four populations on the basis of phases present at room temperature and their freezing/homogenization behaviour. Microthermometric data are summarized in Tables 2A to 2E.

Type I: Low to Moderate Salinity, Liquid Dominated

Type I inclusions are liquid-rich, low to moderate salinity, and they contain liquid + vapour phases. Rarely, one or two translucent daughter minerals (not halite or sylvite) are present. Type I inclusions are sparse in the igneous quartz phenocrysts and in the porphyry-style quartz veins but are common in the skarn, mantos and No. 1 Zone veins.

First melting of ice between -77 and -26°C indicates that salts such as Ca-, Mg- or Fe-chlorides may present in addition to NaCl (Table 2A). Melting of hydrohalite is observed as a sudden clearing in the inclusions in the presence of ice at temperatures of between -42.6 to -15°C . Final ice melting is observed between temperatures of -24 to 0°C . Homogenization to the liquid phase is recorded at temperatures of 339 to 379°C for 2 inclusions in a quartz phenocryst, 354 to 513.3°C for veins in the porphyry, 305 to 444°C for massive sulphide samples from the mantos and 183 to 323°C for the No. 1 Zone veins. Virtually no difference can be distinguished between melting and homogenization temperatures of fluid inclusions from different origins in the porphyry, skarn and manto (Table 2A). Primary fluid inclusions in the No. 1 Zone veins appear to melt initially at lower temperatures and perhaps homogenize at higher temperatures but the paucity of data precludes any real distinction between primary and secondary fluid inclusions.

Type II: Low-Salinity, Vapour Dominated

Type II inclusions appear to be vapour-rich, as they contain vapour + liquid phases, and homogenize to the vapour (with rare exception to the liquid, *see following*). They are common in both the porphyry and No. 1 Zone vein

TABLE 1
SUMMARY DESCRIPTIONS OF SAMPLES USED FOR FLUID INCLUSION MICROTHERMOMETRIC ANALYSES,
LUSTDUST PROPERTY

SAMPLE NUMBER	ZONE	DRILL HOLE 1 2	DEPTH	UTM(E)3	UTM(N)3	DEPOSIT TYPE	HOST ROCK	FEATURE STUDIED	FEATURE TYPE 4 (mineral examined for FI in bold)
GR01-54	porphyry	LD01-34	387 ft	346495	6162133	porphyry	monzonite	vein	qz +ks+py±cp±mg
GR01-60	porphyry	LD01-34	292 ft	346495	6162133	porphyry	monzonite	vein	qz +py
GR01-62	porphyry	LD01-34	232 ft	346495	6162133	porphyry	monzonite	vein phenocryst	qz +mo+py±cp±bo qz
GR01-74	porphyry	LD01-30	847 ft	346484	6161771	porphyry	diorite	vein phenocryst	qz +mo+py±cp±bo qz
GR01-85	porphyry	LD01-36	225 ft	346448	3162051	porphyry	hornfels 48 ft from diorite margin	vein	qz +ks+py±cp±mg
GR01-87	porphyry	LD01-36	332 ft	346448	3162051	porphyry	hb-diorite	vein phenocryst	qz +mo+py±cp±bo qz
GR01-106	porphyry	LD01-30	138.8 ft	346484	6161771	porphyry	hb-diorite	vein phenocryst	qz +to+cpy+py qz
GR01-20	skarn (porphyry?)	LD99-17	275 ft	-	-	skarn		massive skarn	gn +cp+sp+mg (ca)
GR01-31	skarn	LD97-11	289 ft	346827	6161912	skarn	garnet skarn	massive skarn	gn +cp+sp+mg
GR01-61B	skarn	LD01-33	561 ft	346938	6162115	skarn	garnet skarn	massive skarn	gn +cp+sp+mg
GR01-66	skarn	LD20-7	327 ft	347005	6161745	skarn	garnet skarn	massive skarn	gn +(cpx+amp+ca)+c p+py
GR01-47A	4B Zone	LD93-4	90 m	347153	6161265	manto	limestone	massive sulphide	py+po+cp+ qz
GR01-48	4B Zone	LD93-4	91.5 m	347153	6161265	manto	limestone	massive sulphide	py+po+cp+ qz
GR01-104	No. 1 Zone - Takla Silver Mine	-	-	347860	6160518	vein	limestone	vein	py+as+ss+ qz ±sp (ca)
GR01-105	No. 1 Zone - Takla Silver Mine	-	-	347860	6160518	vein	limestone	vein	py+as+ss+ qz ±sp

1. Drill hole year-number; dash = surface grab sample

2. ft = feet, m = metres

3. dash = location uncertain

4. Mineral abbreviations as follows: qz = quartz, py = pyrite, cp = chalcopyrite, gn = garnet, sp = sphalerite, cpx = clinopyroxene, amp = amphibole, ca = carbonate, po = pyrrhotite, as = arsenopyrite, ss = sulphosalt, ks = potassium-feldspar, to = tourmaline

TABLE 2A
SUMMARY DESCRIPTIONS OF SAMPLES USED FOR FLUID INCLUSION MICROTHERMOMETRIC ANALYSES,
LUSTDUST PROPERTY

FEATURE (FEATURE TYPE)	FI ORIGIN 1	FIRST ICE MELT TEMP. range (N) oC (mean ± 1 sig.)	INTERMEDIATE MELT TEMP. 2 range (N) oC (mean ± 1 sig.)	LAST MELT TEMP. 3 range (N) oC (mean ± 1 sig.)	HOMOG. TEMP. range (N) oC (mean ± 1 sig.)
porphyry					
phenocryst (monzonite)	I	-77.4 to -52.2 (2) (-64.8 ± 17.8)	-42.6 (1)	-5.6 (1)	339 to 379 (2) (359 ± 28.3)
phenocryst (diorite)	none noted				
vein (qz+to+cp+py)	PS	-62.9 (1)	-23.8 (1)	-11.6 (1)	not observed
vein (qz+ks+py±cp±mg)	I	-53 to -45 (2) (-49 ± 5.6)	-27 to -25.3 (2) (-26.2 ± 1.2)	-4.3 (1)	489.9 (1)
vein (qz+mo+py±cp±bo)	I	-32.3 (2) (-32.3 ± 0)	-26 (1)	-12.2 to -7.3 (2) (-9.8 ± 3.5)	380.6 to 513.3 (3) (430.6 ± 72.2)
vein (qz+mo+py±cp±bo)	S	-65 to -52.7 (2) (-58.9 ± 8.7)	-27 to -26 (2) (-26.6 ± 0.7)	-16.4 to -7.5 (2) (-12.0 ± 6.3)	467 to 473.9 (2) (470 ± 4.8)
vein (qz+se+py)	I	-37 to -26.6 (2) (-31.8 ± 7.4)	-15 (1)	-7.3 to -6 (2) (-6.7 ± 0.9)	354 to 405.4 (2) (379.7 ± 36.3)
vein (qz+py)	none noted				
skarn					
massive skarn (gn+cp+sp+mg)	P	-55 to -36.5 (7) (-48.7 ± 7.6)	-27.6 to -25.2 (6) (-29.6 ± 3.5)	-16.6 to -7.2 (6) (-13.8 ± 3.6)	not usable
massive skarn (gn+cp+sp+mg)	PS	-40.2 to -54.5 (4) (-43.9 ± 7.1)	-34 to -20.8 (3) (-28.8 ± 7.0)	-17.9 to -13 (4) (-15.3 ± 2.3)	not usable
massive skarn (gn+cp+sp+mg)	S	-45.7 to -39.8 (2) (-42.8 ± 4.2)	-38 to -27 (2) (-32.5 ± 7.8)	-23.6 to -14.8 (2) (-19.2 ± 6.2)	not usable
massive skarn (gn+(cpx+amp+ca)+ cp+py)	P	-40.6 to -39 (2) (-39.8 ± 1.1)	-22.5 (1)	-14.1 to -11 (2) (-12.6 ± 2.2)	not usable
manto					
massive sulphide (py+po+cp+qz)	P	-38.3 to -31.9 (5) (-34.7 ± 2.5)	-27.3 to -21.9 (5) (-25.2 ± 2.5)	-24 to -11.6 (5) (-16.9 ± 4.5)	340 to 444 (6) (386 ± 35.9)
massive sulphide (py+po+cp+qz)	PS	-38.1 to -36.2 (3) (-36.9 ± 1.0)	-28.7 to -28.4 (3) (-28.6 ± 0.2)	-23.9 to -6.1 (4) (-16.2 ± 8.6)	305 to 406 (6) (354.9 ± 33.2)
vein					
massive sulphide (py+as+ss+qz±sp)	P	-64 to -29.3 (5) (-47.7 ± 12.8)	-31 to -26.4 (2) (-28.7 ± 3.3)	-22 to 0 (6) (-9.3 ± 9.9)	218 to 323 (8) (265.7 ± 35.3)
massive sulphide (py+as+ss+qz±sp)	S	-40.5 to -32.9 (3) (-35.4 ± 4.4)	-25 to -15 (2) (-20 ± 7.1)	-11 to -6.1 (3) (-8.0 ± 3)	183 to 309.9 (5) (247.9 ± 48.8)

1. P = primary, PS = pseudosecondary, S = secondary, I = intermediate

2. Assumed to be salt-hydrate (hydrohalite?) melt (see text for description of melting behaviour)

3. Assumed to be last ice melt (see text for description of melting behaviour)

samples. Vapour-rich inclusions from the No. 1 Zone veins homogenize to both vapour (type II) and liquid (type IIQ). The behaviour of the type II inclusions from the veins during heating indicates that they probably represent a single population trapped at near critical conditions.

First and final ice-melting temperatures were difficult to obtain for type II inclusions because of the small amount of liquid present. First melting of ice between -53 and -29.5°C, observed in 6 inclusions, indicates the presence of CaCl₂, MgCl₂ and/or FeCl₃ in addition to NaCl (Table 2B). An intermediate melting event, recorded between -28.6 and -25°C in only 3 inclusions, is interpreted as melting of hydrohalite. Final ice melting is observed between temperatures of -8.8 and -0.4°C. Homogenization to the vapour phase is recorded at temperatures of 333 to 545.6°C in the

igneous quartz phenocrysts, 334°C to 573.3°C for veins in the porphyry and 310 to 391.7°C in the No. 1 Zone vein. Homogenization to the liquid is recorded in a tight cluster within the range of type II inclusions (between 353.6 and 365°C) for 4 vapour-rich type IIQ inclusions. Insufficient data precludes evaluation of differences in melting and homogenization temperature between fluid inclusions of differing origin.

Type III: High-Salinity, Liquid Dominated

Type III inclusions are liquid-rich and contain halite other daughter minerals at room temperature. They are the most abundant type present in the igneous quartz phenocrysts and in quartz veins in the porphyry. Typically they contain liquid, vapour and halite.

TABLE 2B
MICROTHERMOMETRIC DATA FOR AQUEOUS, VAPOUR-RICH TYPE II INCLUSIONS

FEATURE (FEATURE TYPE)	FI ORIGIN ¹	FIRST ICE MELT TEMP. range (N) °C (mean ± 1 sig.)	INTERMEDIATE MELT TEMP. ² range (N) °C (mean ± 1 sig.)	LAST MELT TEMP. ³ range (N) °C (mean ± 1 sig.)	HOMOG. TEMP. range (N) °C (mean ± 1 sig.)	TO PHASE	COMMENT on melt/ homog. behaviour
porphyry							
phenocryst (monzonite)	I				333 (1)	vapour	
phenocryst (diorite)	I	-51.7 (1)	-28.6 (1)	-8.8 (1)	400 to 545.6 (3) (463.9 ± 74.4)	vapour	
vein (qz+to+cp+py)	PS				400 (1)	vapour	
vein (qz+ks+py±cp±mg)	I					vapour	
vein (qz+mo+py±cp±bo)	S	-53 (1)	-23.4 (1)	-5.3 to 3.4 (2) (-1 ± 6.1)	334 to 573.3 (4) (407.7 ± 111.3)	vapour	
vein (qz+se+py)	PS					vapour	
vein (qz+py)	I					vapour	
s karn							none noted
manto							none noted
vein							many cannot observe
massive sulphide (py+as+ss+qz±sp)	P	-48.1 to -32 (2) (-40.1 ± 11.4)	-25 (1)	-2.5 to -0.4 (2) (-1.5 ± 1.5)	337 to 391.7 (6) (362 ± 19.0)	vapour	
massive sulphide (py+as+ss+qz±sp)	P	-32.2 to -29.5 (2) (-30.9 ± 1.9)		-4.7 to -2.4 (4) (-3.4 ± 1.0)	353.6 to 365 (4) (357.2 ± 5.4)	liquid	type IIQ inclusions
massive sulphide (py+as+ss+qz±sp)	S				310 to 325 (2) (317.5 ± 10.6)	vapour	

1. P = primary, PS = pseudosecondary, S = secondary, I = intermediate

2. Assumed to be salt-hydrate (hydrohalite?) melt (*see* text for description of melting behaviour)

3. Assumed to be last ice melt (*see* text for description of melting behaviour)

Type IIIA inclusions form approximately 60% of the type III population in the porphyry samples, and they comprise a vapour bubble with larger diameter than the halite cube. Type IIIA inclusions exhibit halite dissolution at temperatures below liquid-vapour homogenization. Type IIIB inclusions, comprise the remaining 40% of the type III population in the porphyry samples, and exhibit a halite cube with larger diameter than the vapour bubble. Type IIIB inclusions homogenize by halite dissolution after liquid-vapour homogenization. Approximately equal numbers of analyzed type III inclusions homogenize by vapour-bubble disappearance (type IIIA) and halite dissolution (type IIIB), regardless of inclusion origin (Figure 3a). Type III inclusions in the porphyry phenocrysts and veins may contain an opaque mineral (sometimes cubic or hexagonal plate) and/or one or two translucent solids in addition to halite (Photo 1).

Type III inclusions generally exhibit first ice melting between -78 and -40°C, although melting may begin as high as -26°C (Tables 2C and 2D). These observed first melting

temperatures compare with the eutectic temperatures for the CaCl₂-H₂O, NaCl-CaCl₂-H₂O, and FeCl₃-H₂O systems that are -49.8°C, -52°C and -55°C (Linke 1958, 1965), respectively. First melting temperatures below -55°C would require additional components in the fluid inclusions. Last ice melting, in the presence of hydrohalite, is recorded between -50.2 and -21°C (generally between -35 and -21°C). Paucity of data precludes comparison of melting temperatures on the basis of fluid inclusion origin.

Little difference is observed in homogenization temperatures between primary versus secondary fluid inclusions (Figure 3a). Final homogenization temperatures of type IIIA inclusions (by vapour bubble disappearance to the liquid) vary widely from 302.6 to 488°C in quartz phenocrysts, 287 to 635.1°C in veins from the porphyry, 266.8 to 271°C (only 2 inclusions) from quartz in the mantos and 167.4 to 178°C (only 2 inclusions) from quartz from the No. 1 Zone vein (Table 2C, Figure 3b). Final homogenization temperatures of type IIIB inclusions (by halite dissolution to the liquid) also vary widely from 329 to 441.2°C in quartz

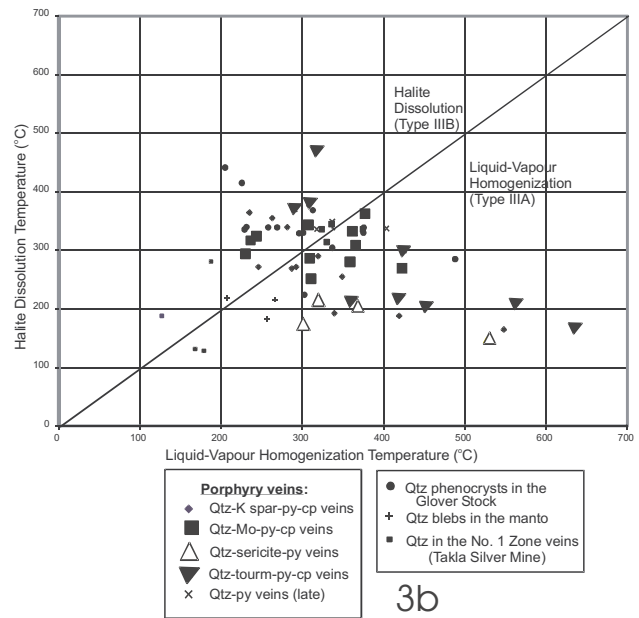
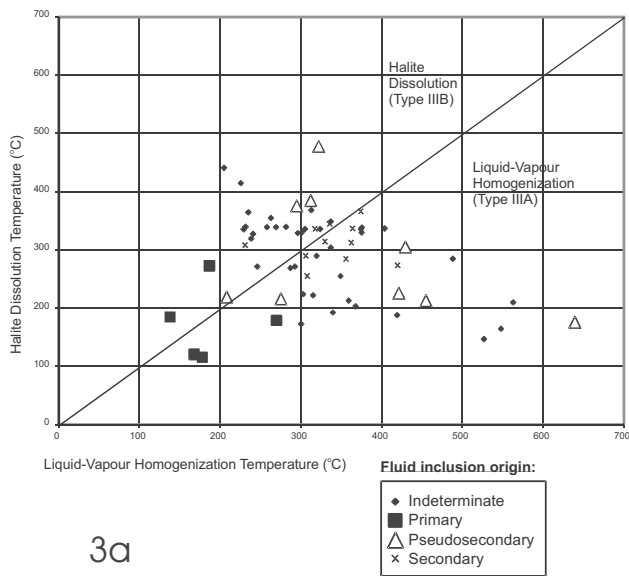


Figure 3. Halite dissolution temperatures as a function of liquid-vapour homogenization temperature for type III inclusions in quartz phenocrysts from the Glover Stock, quartz veins in the porphyry, quartz blebs in massive sulphide from the mantos and quartz from the massive sulphide No. 1 Zone veins, Takla Silver Mine. The diagonal line separates type IIIA from type IIIB inclusions. (a) Temperature of type III fluid inclusions grouped by fluid inclusion origin. Type IIIA and Type IIIB inclusions occur as primary, indeterminate (possibly primary), pseudosecondary and secondary fluid inclusions. (b) Temperature of type III fluid inclusions grouped by deposit and feature type. Type IIIA and Type IIIB inclusions are represented in all deposit/vein types except Qtz-sericite-py veins (Type IIIB only). Note: similar symbols from Figures 3a and 3b do not relate to each other.

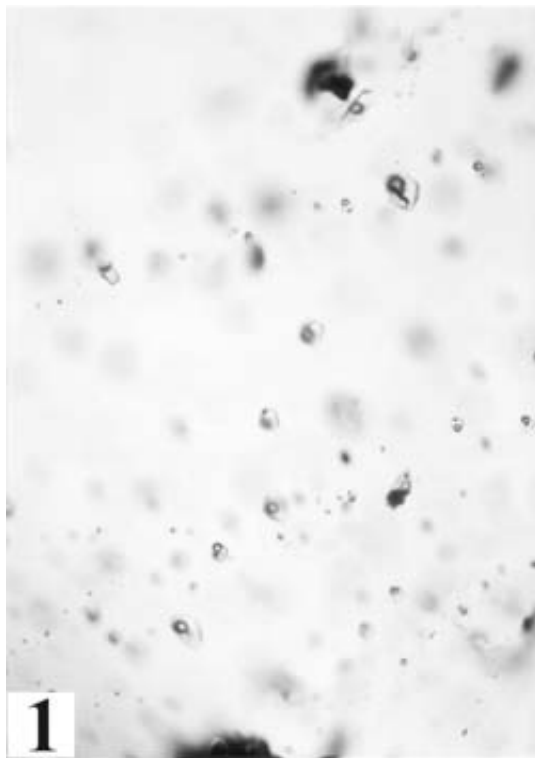


Photo 1. Fracture planes in a Mo-bearing quartz vein from the porphyry defined by secondary type III halite-bearing fluid inclusions, each containing a cubic-shaped, opaque daughter mineral. Sample GR01-60. Transmitted plane light. Long field of view is 0.64 mm.

phenocrysts, 271.5 to 472°C in veins from the porphyry, 213°C (one inclusion) from the mantos, and 189 to 277°C (2 inclusions) from the vein (Table 2D, Figure 3b).

Type IV: Low-Salinity, Vapour Dominated, CO₂-Bearing

Type IV inclusions are vapour-rich, and contain vapour + liquid phases at room temperature. However, CO₂ is detected as a minor, low-density component indicated by phase behaviour at and just below -56.6°C and/or by clathrate formation. Slight depression of the melting point of pure CO₂ (typically less than one degree, Table 2E) indicates trace amounts of CH₄ or N₂. Formation of clathrates (gas-hydrates) at temperatures between -0.5 and +7.9°C indicate that the liquid phase is a low-to-moderate salinity brine. Type IV inclusions are common in the porphyry, manto and No. 1 Zone vein samples. Trace amounts of CO₂ liquid were noted wetting the bubble walls in samples from the mantos and in one sample from the porphyry. This liquid homogenized to the vapour (CO₂ homogenization) a few degrees above clathrate melting (Table 2E).

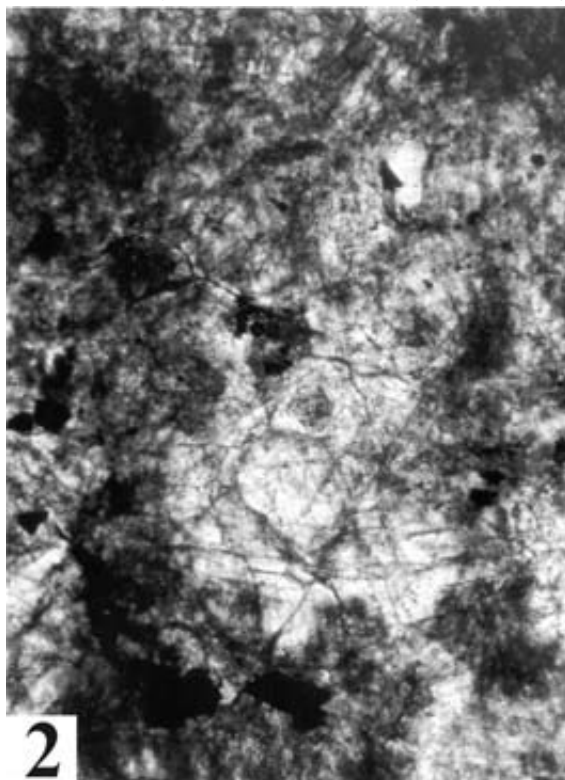
Homogenization to the vapour phase is recorded at temperatures between 351.6 and 378.9°C for quartz phenocrysts, 325 to 552°C from veins in the porphyry, 309 to 385.4°C from quartz in the mantos, and 304 to 357°C (3 inclusions) from the No. 1 Zone vein (Table 2E).

TABLE 2C
MICROTHERMOMETRIC DATA FOR SALT-SATURATED TYPE III INCLUSIONS THAT HOMOGENIZE
BY VAPOUR DISAPPEARANCE (TYPE IIIA)

FEATURE (FEATURE TYPE)	FI ORIGIN ¹	FIRST ICE MELT TEMP. range (N) °C (mean ± 1 sig.)	LAST ICE MELT TEMP. ² range (N) °C (mean ± 1 sig.)	LIQUID-VAPOUR HOMOG. TEMP. (to liquid) range (N) °C (mean ± 1 sig.)	HALITE MELT TEMP. range (N) °C (mean ± 1 sig.)	COMMENT
porphyry						
phenocryst (monzonite)	I	-75 (1)	-33.9 (1)	337 to 488 (4) (393.9 ± 65.3)	285 to 338.8 (4) (314.4 ± 24.6)	opaques common
phenocryst (diorite)	I			302.6 (1)	224 (1)	
vein (qz+to+cp+py)	PS	-36 (1)	-22.5 (1)	417 to 635.1 (4) (481.9 ± 103.1)	168 to 299 (6) (212.4 ± 47.7)	
vein (qz+ks+py±cp±mg)	I	-46 (1)	-27.4 (1)	287 to 419.1 (7) (338 ± 45.0)	188 to 289.8 (7) (239.8 ± 41.3)	opaques common
vein (qz+mo+py±cp±bo)	I	-78 to -69 (4) (-72.3 ± 4.3)	-50.2 to -30 (4) (-39.4 ± 10.9)	300.4 to 526.6 (5) (376.9 ± 89.7)	146.8 to 336 (5) (216.2 ± 72.9)	opaques common
vein (qz+mo+py±cp±bo)	S	-45 to -40 (2) (-42.5 ± 3.5)	-37.6 to -23.4 (2) (-30.5 ± 10.0)	306.4 to 419.9 (7) (356.0 ± 39.4)	255.1 to 366.2 (7) (302.5 ± 38.6)	opaques common
vein (qz+se+py)						none noted
vein (qz+py)	I	-56 (1)	-26 (1)	403.8 (1)	337 (1)	opaque noted
skarn						
none noted						
manto						
massive sulphide (py + po + cp + qz)	P	-26 (1)	-21 (1)	266.8 (1)	183 (1)	
massive sulphide (py + po + cp + qz)	PS	-37 (1)	-21.7 (1)	271 (1)	210 (1)	
vein						
massive sulphide (py+as+ss+qz±sp)	P	-48 to -44 (2) (-46 ± 2.8)	-35 (1)	167.4 to 178 (2) (172.7 ± 7.5)	120 to 122 (2) (121 ± 1.4)	

1. P = primary, PS = pseudosecondary, S = secondary, I = intermediate

2. Last ice melting observed before final melting of salt-hydrate (presumed to be hydrohalite)



TEMPORAL RELATIONSHIPS BETWEEN POPULATIONS

Definitive criteria for primary origin, such as the presence of inclusions in growth zones or geometric arrays of fluid inclusions oriented parallel to crystal faces, were observed in the following mineral assemblages:

- Subhedral 'cloudy' quartz crystal aggregates comprise the gangue (possibly secondary) to sulphide and sulphosalt minerals in the No. 1 Zone veins. Distinct core zones in many of the quartz crystals are characterized by abundant coexisting type I-II-III and type I-IV-III fluid inclusions (Photo 2). Leitch (2001) notes that core zones cut across crystal boundaries in sample GR01-26 from the No. 1 Zone veins. He suggests that original larger, zoned crystals up to 4mm across may have been recrystallized. Some of the core zone type II and IV fluid inclusions exhibit final homogenization to the liquid phase and may have formed at near-critical conditions.
- Subhedral to euhedral quartz occurs interstitial to massive pyrrhotite, pyrite and chalcopyrite in the manto samples. The quartz may be secondary (formed after the

Photo 2. Distinct core zones defined by primary fluid inclusions in quartz crystal aggregates from the No. 1 veins, Takla Silver Mine. Sample GR01-105. Transmitted plane light. Long field of view is 2.63 mm.

TABLE 2D
MICROTHERMOMETRIC DATA FOR SALT-SATURATED TYPE III INCLUSIONS THAT HOMOGENIZE
BY HALITE DISSOLUTION (TYPE IIIB)

FEATURE (FEATURE TYPE)	FI ORIGIN ¹	FIRST ICE MELT TEMP. range (N) °C (mean ± 1 sig.)	LAST ICE MELT TEMP. ² range (N) °C (mean ± 1 sig.)	LIQUID-VAPOUR HOMOG. TEMP. (to liquid) range (N) °C (mean ± 1 sig.)	HALITE MELT TEMP. range (N) °C (mean ± 1 sig.)	COMMENT
porphyry						
phenocryst (monzonite)	I			258 to 301 (3) (285 ± 23.5)	329 to 339 (3) (332.7 ± 5.5)	opaques common
phenocryst (diorite)	I		-27.3 (1)	205 to 313 (6) (245.6 ± 39)	335.4 to 441.2 (6) (373.1 ± 44.9)	
vein (qz+to+cp+py)	PS			290.6 to 318 (3) (305.5 ± 13.9)	370.1 to 472 (3) (407 ± 56.4)	opaques common
vein (qz+ks+py±cp±mg)	I			234.9 to 281.5 (4) (256.3 ± 20.4)	271.5 to 364.7 (4) (332.7 ± 42.1)	
vein (qz+mo+py±cp±bo)	I	-74.5 (1)	-49 (1)	240.7 to 324 (4) (277 ± 44)	319.6 to 336 (4) (329.8 ± 7.9)	opaques common
vein (qz+mo+py±cp±bo)	S			231 to 335.8 (3) (298.9 ± 58.9)	308 to 344.8 (3) (322.3 ± 19.7)	
vein (qz+se+py)						none noted
vein (qz+py)	I			337 (1)	349 (1)	
vein (qz+py)	S			318 (1)	336 (1)	
skarn						
none noted						
manto						
massive sulphide (py + po + cp + qz)	PS			204 (1)	213 (1)	
vein						
massive sulphide (py+as+ss+qz±sp)	P			135 to 183.5 (2) (159.3 ± 34.3)	189 to 277 (2) (233 ± 62.2)	

1. P = primary, PS = pseudosecondary, S = secondary, I = intermediate

2. Last ice melting observed before final melting of salt-hydrate (presumed to be hydrohalite)

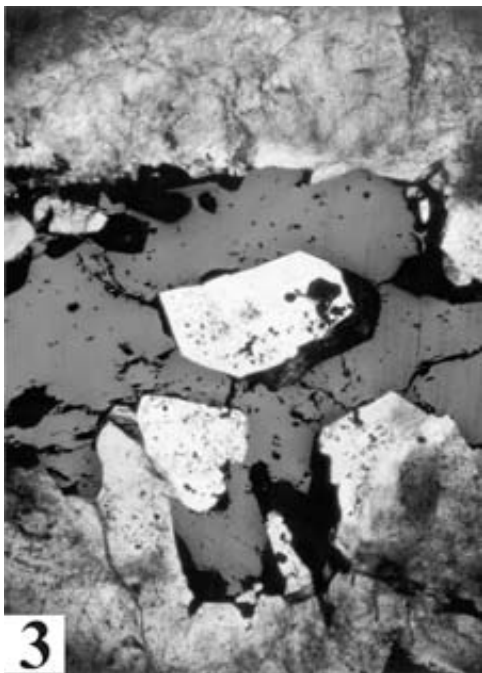


Photo 3. Geometric arrays of primary fluid inclusions in subhedral to anhedral quartz (light minerals) occurring interstitial to massive pyrrhotite (grey minerals) in the manto (No. 4B Zone). Sample GR01-48. Transmitted and reflected light. Long field of view is 2.63 mm.

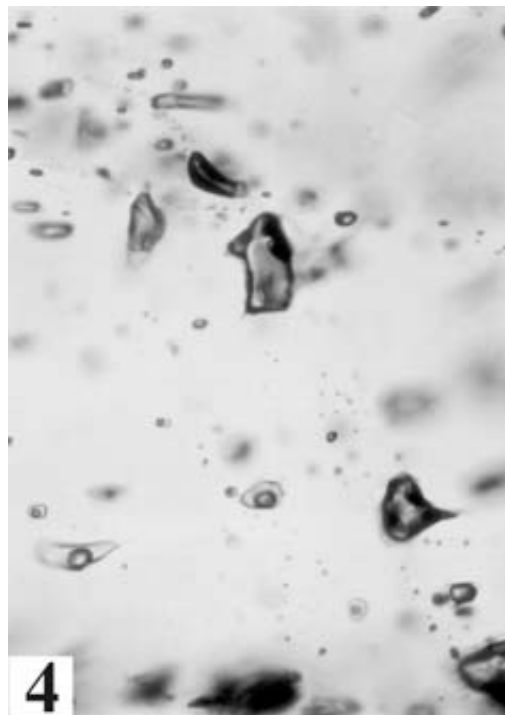


Photo 4. Coexisting liquid-rich type I and vapour-rich type IV primary fluid inclusions in quartz from No. 4B Zone mantos. Sample GR01-47A. Transmitted plane light. Long field of view is 160 µm.

TABLE 2E
MICROTHERMOMETRIC DATA FOR CARBONIC, VAPOUR-RICH TYPE IV INCLUSIONS

FEATURE (FEATURE TYPE)	FI ORIGIN ¹	CO ₂ MELT TEMP. range (N) °C (mean ± 1 sig.)	LAST ICE MELT TEMP. range (N) °C (mean ± 1 sig.)	CLATHRATE MELT TEMP. (to liquid) range (N) °C (mean ± 1 sig.)	CO ₂ HOMOG. TEMP. range (N) °C (mean ± 1 sig.)	TO PHASE	FINAL HOMOG. TEMP. (to vapour) range (N) °C (mean ± 1 sig.)	COMMENT
porphyry								
phenocryst (monzonite)	I	-56.8 to -56.6 (3) (-56.7 ± 0.1)	-9 to -3.5 (2) (6.3 ± 3.9)	-0.5 to 5.8 (3) (3.5 ± 3.5)			351.6 to 378.9 (2) (365.3 ± 19.3)	
phenocryst (diorite)								none noted
vein (qz+to+cp+py)	PS	-59.9 (1)	-6.6 (1)	6.2 (1)			325 (1)	
vein (qz+ks+py±cp±mg)	I	-58.9 to -56.6 (6) (-57.2 ± 0.9)	-15 to -2.2 (5) (-10.5 ± 5)	4.7 (1)			366 to 494 (6) (448.1 ± 49.4)	
vein (qz+mo+py±cp±bo)	I	-56.9 to -56.6 (5) (-56.7 ± 0.1)	-10.8 to -0.9 (4) (-3.6 ± 3)	-3.1 to 5.1 (4) (1.6 ± 3.1)			347 to 412 (6) (368.3 ± 26.5)	
vein (qz+mo+py±cp±bo)	S	-56.9 (1)	-10.8 (1)	-3.1 (1)			347 (1)	
vein (qz+se+py)	S	-57.4 (1)	-5.2 to -4.4 (2) (-4.8 ± 0.6)	-0.2 to 1.3 (2) (0.5 ± 1.1)			367.1 to 377 (2) (372 ± 7)	
vein (qz+py)	PS	-57.1 (1)					552 (1)	
skarn								
none noted								
mantle								
massive sulphide (py+po+cp+qz)	P	-58.3 to -57.2 (3) (-57.6 ± 0.6)	1.1 (1)	2.3 to 7.9 (3) (5.1 ± 2.8)	4 to 11.4 (3) (8.5 ± 3.9)	vapour	309 to 385.4 (3) (353.5 ± 39.7)	
massive sulphide (py+po+cp+qz)	PS	-57.3 to -58.3 (3) (-57.8 ± 0.5)		0.2 to 6 (3) (2.4 ± 3.1)	3.1 to 10.6 (3) (7.4 ± 3.9)	vapour	315 to 354 (3) (329.7 ± 21.2)	
vein								
massive sulphide (py+as+ss+qz±sp)	P	-56.6 (2)	-4.1 to -2.3 (2) (-3.2 ± 1.3)	3.4 to 7.6 (3) (4.9 ± 2.3)			304 to 328 (2) (316 ± 17)	
massive sulphide (py+as+ss+qz±sp)	S	-56.8 (1)		3.6 (1)			357 (1)	

1. P = primary, PS = pseudosecondary, S = secondary, I = intermediate



Photo 5. Growth zones in skarn garnet. Zones are defined by large, irregular-shaped type I fluid inclusions. Sample GR01-31. Transmitted plane light. Long field of view is 2.63 mm.

sulphide minerals). It contains geometric arrays of fluid inclusions oriented parallel to crystal faces (Photo 3). Co-existing types I and IV fluid inclusions characterize the fluid inclusion assemblages in the arrays (Photo 4).

- Zoned garnet crystals in the skarn contain large, irregular-shaped Type I fluid inclusions that define growth zones (Photo 5). The very large, structurally-weak inclusions (~100 microns) have decrepitated (even when 250 micron thick sections were used for observation). The large size, irregular shape and mostly inconsistent liquid-to-vapour ratios of these primary inclusions suggest that they necked down and underwent post-entrapment change in mass and/or volume. Homogenization temperatures from these primary inclusions are unreliable but the salinity values are believed to be valid.
- Primary growth bands were observed in quartz from a 6 mm thick molybdenite-pyrite-bearing quartz veinlet in the porphyry. Fluid inclusions within the growth bands could not be distinguished, as they are less than 1 micron in maximum size. No other evidence of primary origin was noted in the porphyry.

Pseudosecondary and secondary fluid inclusions occurring along fracture planes were observed in samples from the skarn, mantos and No. 1 Zone veins. Definitive fluid inclusion fracture planes were observed in a few quartz veins from the porphyry. The majority of fluid inclusions in quartz from porphyry veins and phenocrysts occur as 'clus-

ters', or are 'isolated'. These inclusions have been assigned an indeterminate origin.

Temporal relationships between secondary and indeterminate populations are subtle and will require observation of additional samples to resolve. However, the following observations are noted:

- (a) Type II, III and IV inclusions are dominant in the porphyry (type II less abundant) and coexist in both quartz phenocrysts and veins. Fracture planes with coexisting type IIIA and IV fluid inclusions (Photo 6) are common. These fractures crosscut fracture planes with only type IIIB fluid inclusions in sample GR01-106. Type II inclusions can comprise isolated fracture planes (photo 7). Less commonly, Type II or IV inclusions coexist with Type I inclusions in "clusters" of indeterminate origin.
- (b) In the skarn garnets, secondary type I fluid inclusions are much smaller than the primary and pseudosecondary inclusions and have smooth to negative-crystal shapes. Fluid inclusion assemblages with variable liquid-to-vapour ratios indicate necking down, consequently, the homogenization temperatures were not used in this study.
- (c) In the mantos, pseudosecondary type I and lesser type IV fluid inclusions coexist (Photo 4). Where rare type III fluid inclusions were noted, they sometimes coexist with type I inclusions.
- (d) Secondary type I and type II or IV fluid inclusions coexist in the No. 1 Zone veins, but secondary type III inclusions have not been noted.

FLUID INCLUSION COMPOSITIONS

Petrographic and microthermometric data of fluid inclusions from the porphyry, skarn, mantos and No. 1 Zone veins indicate four fluid inclusion populations which can be modeled as varieties of two types of fluids: $H_2O - NaCl - CaCl_2$ ($\pm FeCl_3, MgCl_2$) and $H_2O - CO_2 - NaCl - CH_4$.

$H_2O - NaCl - CaCl_2$ ($\pm FeCl_3, MgCl_2$) Fluids

The dominant salt components in the vast majority of naturally-occurring fluids are NaCl, $CaCl_2$, KCl, $MgCl_2$ and $FeCl_2$ (Shepherd *et al.*, 1985, p. 101). At Lustdust, the ternary $H_2O - NaCl - CaCl_2$ system is used to model type I, II and III fluid inclusions for a number of reasons. First, the eutectic (first melting) temperatures for these inclusions are typically < -35 to $40^\circ C$ (Tables 2A through 2D), which indicates the presence of possible Ca-, Mg- or Fe- chlorides. In fact, first melting temperatures as low as $-73^\circ C$ are reported in synthetic $NaCl - CaCl_2 - H_2O$ inclusions (Vanko *et al.*, 1988, p. 2454) although temperatures this low are usually attributed to additional components. Second, there is little evidence for KCl (no sylvite daughter minerals and first melting $< -22.9^\circ C$). Third, KCl and $MgCl_2$ are relatively minor components of most fluids (Shepherd *et al.*, 1985) and $FeCl_2$ is not a common chloride species (Goldstein and Reynolds, 1994, Table 7.2 modified from Crawford, 1981). Finally, the physical properties of $CaCl_2$ and $MgCl_2$ hy-

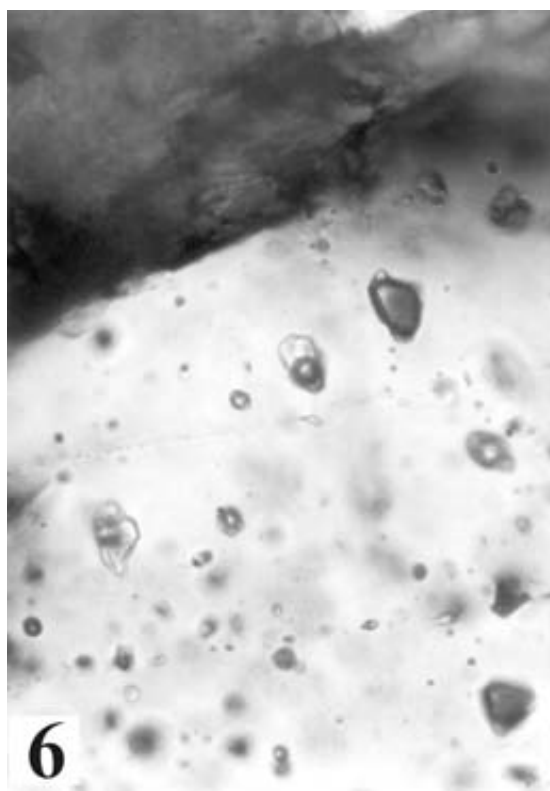


Photo 6. Coexisting halite-bearing type III and vapour-rich type IV fluid inclusions of indeterminate origin in quartz from a Mo-bearing quartz porphyry vein in the Glover Stock. Sample GR01-87. Transmitted plane light. Long field of view is $160 \mu m$.



Photo 7. Fracture planes in quartz from a Mo-bearing quartz porphyry vein in the Glover Stock. Planes are defined by secondary vapour-rich type II fluid inclusions only. Sample GR01-60. Transmitted plane light. Long field of view is $0.64 mm$.

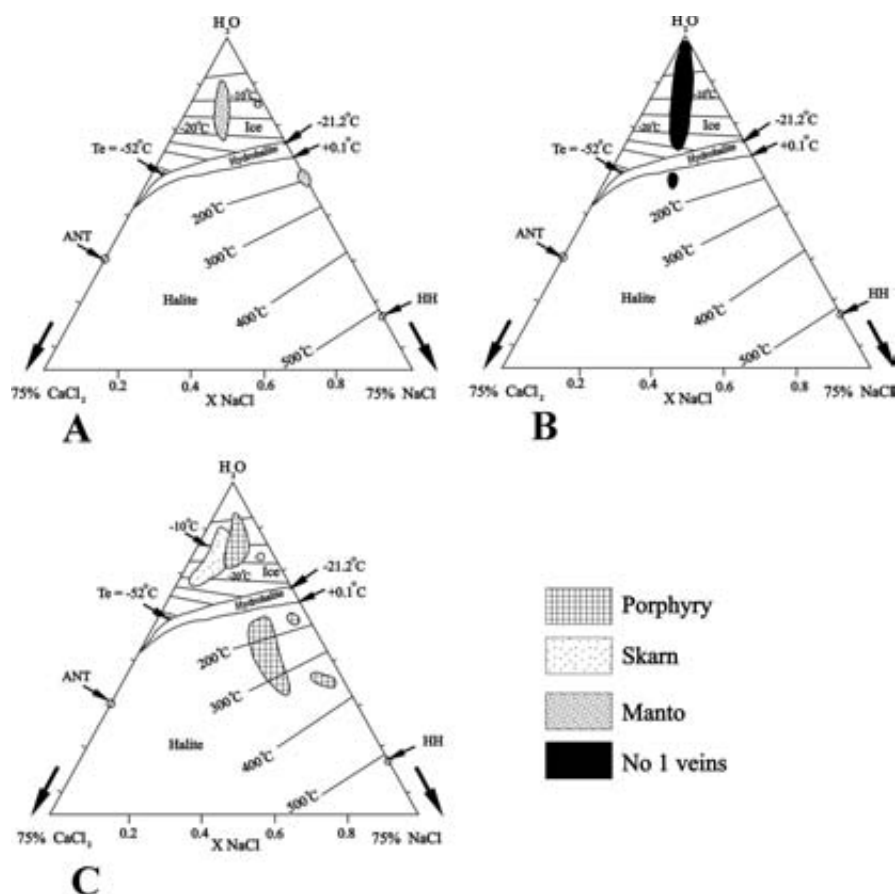


Figure 4. Phase diagrams showing liquidus relations in the ternary system NaCl-CaCl₂-H₂O with compositions in weight percent (from Oakes *et al.* 1990 and Vanko *et al.* 1988). The compositional ranges of fluid inclusions in (A) quartz in massive sulphide from the mantos, (B) quartz from the massive sulphide veins at the Takla Silver Mine, (C) porphyry quartz veins and garnet skarn. HH = hydrohalite (NaCl.2H₂O), ANT = antarcticite (CaCl₂.6H₂O).

drates are similar and most aqueous fluids are well represented by the ternary H₂O-NaCl-CaCl₂ system (Shepherd *et al.*, 1985).

Assuming an H₂O-NaCl-CaCl₂ model system, hydrohalite melting, in the presence of ice, liquid and vapour, is used to estimate the weight fraction of NaCl (XNaCl) for type I and type II inclusions (method of Oakes *et al.*, 1990, Figure 4). Ice melting, in the presence of hydrohalite, liquid and vapour is used to estimate XNaCl for type III inclusions (method of Vanko *et al.*, 1988, Figure 4). In type III inclusions where halite never transformed to hydrohalite on cooling, measurements of ice melting in the presence of liquid, vapour and metastable halite were also used to crudely estimate the bulk composition.

Distinct ranges of XNaCl are apparent in the Lustdust porphyry, skarn, manto and vein fluids (Figure 4). Porphyry, skarn and manto fluids record two ranges of XNaCl corre-

sponding evidence for both NaCl-dominant fluids (> 0.8 XNaCl) and mixed NaCl-CaCl₂ fluids (< 0.7 XNaCl, Table 3). The difference between the various ranges is not attributable to inclusion origin or type.

Final ice melting is used to estimate the total salinity of type I and II inclusions (method of Oakes *et al.*, *op. cit.*, Figure 4). Ice melting and halite dissolution temperatures are used to determine the bulk composition of type III inclusions (method of Vanko, 1988). The total salinity (weight % salts) ranges in weight percent salts for mixed NaCl-CaCl₂ fluids and the total salinity ranges in weight percent salts for NaCl-dominant fluids are in Table 3. In general, the NaCl-dominant fluids have higher salinities than most of the mixed NaCl-CaCl₂ fluids.

TABLE 3
FLUID INCLUSION COMPOSITIONS, LUSTDUST PROSPECT

DEPOSIT TYPE	H ₂ O-NaCl-CaCl ₂ (± FeCl ₃ , MgCl ₂) FLUIDS				H ₂ O-CO ₂ -NaCl-CH ₄ FLUIDS				
	mixed NaCl-CaCl ₂ FLUIDS		NaCl-dominant FLUIDS		aqueous phase	bulk fluid			
	X NaCl	wt. % salts	X NaCl	wt. % salts	eq. wt. % NaCl	X NaCl	XH ₂ O	XCO ₂	XCH ₄
igneous phenocrysts	0.4, 0.65*	13, 40*			7.7 to 16.1				
porphyry veins	0.4 to 0.7	6 to 51	0.8 to 1	28 to 44	7.0 to 18.4				
prograde skarn	0.1 to 0.5	9 to 22							
retrograde skarn			0.8	17					
manto	0.3 to 0.4	15 to 24	0.8 to 1	23 to 30	4.1 to 14.3	0.01 to 0.05	0.73 to 0.89	0.06 to 0.21	0 to 0.03
Takla Silver veins	0.3 to 0.6	2 to 31			2.1 to 4.6				

* Based on 2 samples, points not plotted on Figure 4.

H₂O-CO₂-NaCl-CH₄ Fluids

The identification of CO₂ in type IV fluids at Lustdust is based upon clathrate melting between -0.5 and +7.9°C, less commonly by phase behaviour at or just below -56.6°C (pure CO₂ melting point), and rarely, in fluid inclusions from the mantos, by wetting of bubble walls by tiny amounts of CO₂ liquid. Because liquid CO₂ was observed in only trace amounts, the CO₂ is presumed to exist as a gas in the inclusion bubble and as a minor aqueous component.

Salinity estimates for type IV inclusions (eq. wt. % NaCl) based on clathrate melting were calculated using the H₂O-CO₂-NaCl-CH₄ system (Jacobs and Kerrick, 1981; Brown and Hagemann, 1994).

Salinities from type IV fluid inclusions in the mantos are much lower than those recorded for H₂O-NaCl-CaCl₂ (±FeCl₃, MgCl₂) fluids (Table 3). CO₂ homogenization to vapour, indicating a low-density CO₂ phase, was extremely difficult to observe and only observed in samples from the mantos; it seemed to occur a few degrees above clathrate melting. Bulk compositions of type IV fluid inclusions from the mantos are included in Table 3.

ESTIMATED TRAPPING CONDITIONS

A variety of methods were used to estimate *minimum* trapping pressures of the fluid inclusions in the porphyry, skarn, mantos and No. 1 Zone veins. These methods involve the construction of isochores using fluid inclusion microthermometric data for the H₂O-NaCl and H₂O-CO₂-NaCl-CH₄ systems. The H₂O-NaCl model system is used to construct isochores for the H₂O-NaCl-CaCl₂ (±FeCl₃, MgCl₂) fluids because the pressure-temperature-compositional properties of the latter more complex system are unknown. This substitution is reasonable based on work by Potter and Cline (1978). Their work demonstrates that the volumetric properties of many Na-K-Ca-Mg-Br-SO₄ brines are within ±1% of those of an NaCl solution having the same depression of freezing point. Thus, the isochores of aqueous liquid-vapour fluid inclusions in many multi-component systems will be the same as those for H₂O-NaCl provided that the comparison is on the basis of NaCl equivalent obtained by freezing point depression. However, the actual salinities will be different and the equivalent weight % NaCl will not equal total weight % salts.

TABLE 4
SUMMARY OF PRESSURE ESTIMATES AND TRAPPING CONDITIONS

FEATURE (FEATURE TYPE)	TRAPPING PRESSURE BASED ON CONDITIONS OF FLUID IMMISCIBILITY (bars)		MINIMUM TRAPPING PRESSURE BASED ON		DEPTH ESTIMATE ASSUMING	
	Type IIIA or Type I ¹	Type IV ²	HOMOGENIZATION BY HALITE DISSOLUTION (bars) ³	TRAPPING AT NEAR-CRITICAL CONDITIONS (bars)	LITHOSTATIC PRESSURE REGIME	HYDROSTATIC PRESSURE REGIME ³
porphyry						
phenocryst (monzonite)	150	~500 est.	880		570 metres? ~1.9 km	1.5 km? ~5.1 km
phenocryst (diorite)			880		3.3 km	9.0 km
vein (qz+to+cp+py)			1800*		3.3 km	9.0 km
vein (qz+ks+py±cp±mg)			950		6.8 km*	18 km*
vein (qz+mo+py±cp±bo)	150	450 to 500 est.			3.6 km	9.7 km
vein (qz+se+py)	120	~450 to 500 est.	230		570 metres? ~1.7 to 1.9 km	1.5 km? ~4.6 to 5.1 km
vein (qz+py)			260		870 metres	2.3 km
manto					450 metres	1.2 km
massive sulphide (py+po+cp+qz)		320			~1.7 to 1.9 km	~4.6 to 5.1 km
vein					980 metres	2.7 km
massive sulphide (py+as+ss+qz±sp)			170	300 to 400	1.2 km 640 metres	3.3 km 1.7 km
			1700*		1.1 to 1.5 km 6.4 km*	3.1 to 4.1 km 17 km*

1. Pressure estimates based on isochores and final homogenization to liquid phase for type IIIB inclusions

2. Minimum pressure estimates based on estimated composition of 2 mol % CO₂ (minimum), 10 wt. % NaCl and final homogenization to vapour phase for type IV inclusions

3. * = Minimum pressure and depth estimates seem unreasonably high (see discussion and summary)

Evidence for immiscible entrapment (coexisting NaCl-saturated inclusions or under-saturated inclusions and vapour-rich inclusions which homogenize at the same temperature) is used to calculate estimated *actual* trapping pressures where possible. Evidence for entrapment of vapour-rich fluid inclusions under near critical conditions is also used to estimate trapping pressures. Geologic estimates of inclusion trapping pressures based on paleodepth or the use of mineral geobarometers have not been calculated.

Pressure estimates and depths of emplacement of fluid inclusions calculated using the following methods are summarized in Table 4.

Evidence for and Trapping Conditions of Phase Separation (Immiscibility)

Evidence for immiscible entrapment is abundant in samples from the porphyry. It was observed in fluid inclusion assemblages of indeterminate (possibly primary) origin from quartz phenocrysts in the monzonite and from the following vein types in the porphyry: quartz+potassium feldspar+pyrite±chalcopyrite±magnetite, quartz + molybdenite+pyrite±chalcopyrite±bornite and quartz+sericite+pyrite. Immiscible entrapment was also observed in planes of secondary inclusions from the quartz + molybdenite + pyrite±chalcopyrite±bornite veins. Outside the porphyry, immiscible entrapment was only observed in quartz from one sample of the mantos. Coexisting liquid and vapour-rich inclusions do occur in quartz in the No. 1 Zone veins but they do not homogenize at the same temperature.

Quartz Phenocrysts in the Monzonite Porphyry

Coexisting type IIIA and type IV fluid inclusions occur as isolated clusters in quartz phenocrysts in the monzonite. Homogenization temperatures, type IIIA to the liquid and type IV to the vapour, for the fluid inclusion assemblages are both at $334\pm 10^\circ\text{C}$ and $377\pm 3^\circ\text{C}$ for samples GR01-62 and GR01-60 respectively. Isochores have been calculated for type IIIA inclusions using equations from Bodnar and Vityk (1994) and the computer program MacFlinco (Brown and Hagemann, 1994). Pressures of trapping based on final homogenization by disappearance of the vapour bubble are approximately 100 bars for sample GR01-62 and 150 bars for sample GR01-60. It is not possible to calculate isochores for the type IV fluid inclusions as CO_2 homogenization was not observed in these inclusions precluding density estimates. Estimates of salinity of the liquid phase for type IV inclusions are 7.7 and 8.5 equivalent weight percent NaCl using clathrate melting temperatures.

The observed melting behaviour of type IV inclusions suggests they contain a low-density, gas-rich fluid, which is probably conjugate to the briny type III inclusions (based on very similar homogenization temperatures for both types of fluids). Phase separation of type III and IV fluids is inferred at maximum pressures of 150 bars and 377°C (using Type IIIA isochore construction and final homogenization data, Table 4). Estimated depths of emplacement based on this pressure estimate are 570 metres under lithostatic load or 1.5 km under hydrostatic load, but neither estimate seems realistic in comparison with the deeper vertical positions of

magmatic (early) fluid inclusions in many porphyry copper deposits (Bodnar, 1995, figure 3). If the presence of perhaps as little as 2 mol % CO_2 in combination with a 10 wt % NaCl aqueous fluid is considered for type IV inclusions from quartz phenocrysts in the monzonite, the vapour pressure at 377°C can be estimated at 500 bars (using figure 9 of Bowers and Helgeson, 1983) which corresponds to more realistic trapping depths of 1.9 km under lithostatic load (Table 4).

Porphyry Veins Associated with Potassium Silicate Alteration±Chalcopyrite

In sample GR01-85 coexisting types I and II fluid inclusions of indeterminate origin homogenize to both liquid and vapour phases at $491\pm 1^\circ\text{C}$ (fluid inclusion assemblage 3-1). Unfortunately, the salinity (eq. wt. % NaCl) for inclusions in this assemblage cannot be calculated since inclusions exhibit ice melting above 0°C . Similar type I inclusions in another assemblage (1-3) from the same sample yield salinities of ~7 eq. wt. % NaCl, however, homogenization temperatures for this assemblage were not recorded and the assemblage did not provide evidence for immiscibility.

Porphyry Veins Associated with Molybdenite ± Chalcopyrite Mineralization

In sample GR01-60, types III and IV fluid inclusions coexist in a fluid inclusion assemblage of indeterminate origin. Homogenization temperatures to both liquid (type IIIA) and vapour (type IV) are $366\pm 11^\circ\text{C}$. Isochores have been calculated for type IIIA inclusions using equations from Bodnar and Vityk (1994) and the computer program MacFlinco (Brown and Hagemann, 1994). Pressures of trapping based on final homogenization by disappearance of the vapour bubble in type IIIA inclusions are approximately 150 bars. Absence of observed CO_2 homogenization temperatures precludes density estimates and isochore construction. Using the clathrate melting temperature, the salinity of the liquid phase for type IV inclusions is 8.8 equivalent weight percent NaCl.

In sample GR01-60, types III and IV fluid inclusions and separate type IIIA and II fluid inclusions coexist in fluid inclusion assemblages of secondary origin (FIA's 3-1 and 2-1, respectively). Homogenization temperatures for assemblages 3-1 and 2-1 are $351.5\pm 6.4^\circ\text{C}$ and $370.6\pm 5.4^\circ\text{C}$ respectively. Isochores have been calculated for type IIIA inclusions using equations from Bodnar and Vityk (1994) and the computer program MacFlinco (Brown and Hagemann, 1994). Pressures of trapping based on final homogenization by disappearance of the vapour bubble for type IIIA inclusions are approximately 120 bars and 150 bars for assemblages 3-1 and 2-1 respectively. Absence of observed CO_2 homogenization temperatures for assemblage 3-1 precludes density estimates and isochore construction for type IV inclusions. Using the clathrate melting temperature, the salinity of the liquid phase for type IV inclusions in assemblage 3-1 is 18.4 equivalent weight percent NaCl. The salinity (eq. wt. % NaCl) for type II inclusions in assemblage 2-1 cannot be calculated since inclusions exhibit ice melting above 0°C .

The observed melting behaviour of type IV inclusions of indeterminate (possibly primary) and secondary origin suggests they contain a low-density, gas-rich fluid which is probably conjugate to the briney type III inclusions (based on very similar homogenization temperatures for both types of fluids). Phase separation of type III and IV fluids is inferred at maximum pressures of 150 bars and temperatures of 366°C for inclusions of indeterminate origin and at slightly lower pressures of 120 bars and temperatures of 351.5°C for inclusions of secondary origin. Estimated depths of emplacement for indeterminate and secondary fluids are 570 metres and 450 metres under lithostatic load or 1.5 km and 1.2 km under hydrostatic load (Table 4). If the presence of as little as 2 mol % CO₂ in combination with a 10 wt % NaCl or 20 wt. % NaCl aqueous fluid is considered for type IV inclusions from molybdenite-bearing veins in the porphyry, the vapour pressure at 351 to 366°C is ~450 to 500 bars (using figure 9 of Bowers and Helgeson, 1983) which corresponds to trapping depths of 1.7 to 1.9 km under lithostatic load (Table 4).

Phase separation of type II and III fluids of secondary origin is inferred at maximum pressures of 150 bars and 370°C. Estimated depths of emplacement for these fluids are 570 metres under lithostatic load or 1.5 km under hydrostatic load. There is no evidence for CO₂ in these secondary fluid inclusion assemblages.

Porphyry Veins Associated with Sericite Alteration

In sample GR01-62, types I and IV fluid inclusions coexist in a fluid inclusion assemblage of indeterminate origin. Homogenization temperatures to both liquid (type I) and vapour (type IV) are 360.6±9.3°C. Isochores have been calculated for type I inclusions using equations from Bodnar and Vityk (1994) and the computer program MacFlincon (Brown and Hagemann, 1994). Pressures of trapping based on final homogenization by disappearance of the vapour bubble in type I inclusions are approximately 120 bars. Absence of observed CO₂ homogenization temperatures for type IV inclusions precludes density estimates and isochore construction. Using the clathrate melting temperature, the salinity of the liquid phase for type IV inclusions is 14.1 equivalent weight percent NaCl.

The observed melting behaviour of type IV inclusions of indeterminate (possibly primary) and secondary origin suggests that they contain a low-density, gas-rich fluid which is probably conjugate to the low salinity (9.2 eq. wt. % NaCl) type I inclusions (based on very similar homogenization temperatures for both types of fluids). Phase separation of types I and IV fluids is inferred at maximum pressures of 120 bars and temperatures of 360°C for these inclusions of indeterminate origin. Estimated depths of emplacement are 450 metres under lithostatic load or 1.2 km under hydrostatic load (Table 4). If the presence of as little as 2 mol % CO₂ in combination with a 10 wt % NaCl or 20 wt. % NaCl aqueous fluid is considered for type IV inclusions from molybdenite-bearing veins in the porphyry, the vapour pressure at 360°C is ~450 to 500 bars (using figure 9 of Bowers and Helgeson, 1983) which corresponds to trapping depths of 1.7 to 1.9 km under lithostatic load (Table 4).

Massive Sulphide from the Mantos

In sample GR01-47A, types I and IV fluid inclusions coexist in fluid inclusion assemblage 3-1 of pseudosecondary origin. Homogenization temperatures to both liquid (type I) and vapour (type IV) are 352.5±1.5°C. Isochores have been calculated for all type IV inclusions from the mantos using equations from Jacobs and Kerrick (1981) and the computer program MacFlincon (Brown and Hagemann, 1994). The minimum pressure of trapping based on final homogenization by disappearance of the liquid rim (*i.e.* to the vapour) from assemblage GR01-47A 3-1 is approximately 320 bars (Figure 5). The minimum pressure range for all measured type IV inclusions in sample GR01-47A is from 304 to 386 bars (Figure 5); type IV inclusions from sample GR01-48 have minimum pressure estimates of between 256 and 460 bars (Figure 5). The salinity (eq. wt. % NaCl) for type I inclusions in FIA 3-1 cannot be calculated since inclusions exhibit ice melting below the NaCl-H₂O eutectic of -20.8°C. This implies a high salinity for the type I inclusions and the existence of halite as a daughter mineral. No solid daughter minerals were observed in fluid inclusion assemblage 3-1.

Phase separation of type I and IV fluids is inferred at minimum pressures of 320 bars and temperatures of approximately 350°C for inclusions in FIA 3-1 from sample GR01-47A. Estimated depths of emplacement are 1.2 km under lithostatic load or 3.3 km under hydrostatic load (Table 4).

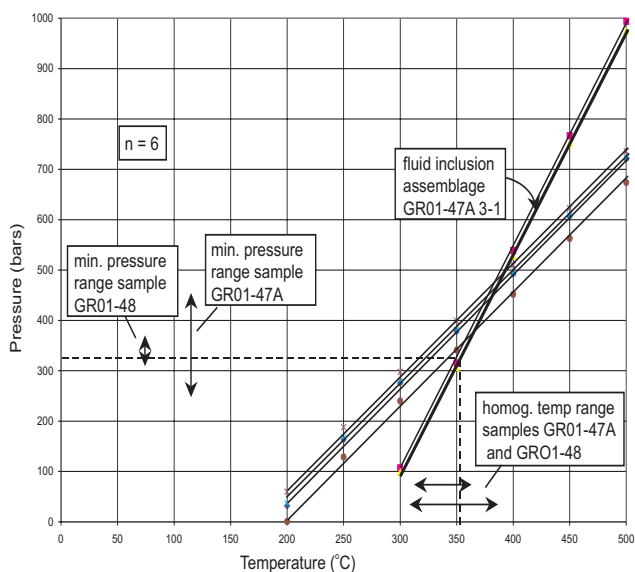


Figure 5. Isochores calculated using the H₂O-CO₂-NaCl-CH₄ system (Jacobs and Kerrick, 1981) and the computer program MacFlincon (Brown and Hagemann, 1995) for type IV inclusions in quartz associated with massive sulphide in the mantos at the Lustdust property. The estimated trapping pressure of coexisting vapour-rich type IV and liquid-rich type I inclusions in sample GR01-47A (fluid inclusion assemblage 3-1) at 352°C is approximately 320 bars (dashed lines). Minimum pressure and homogenization temperature (homog. temp) ranges for samples GR01-47A and GR01-48 are indicated.

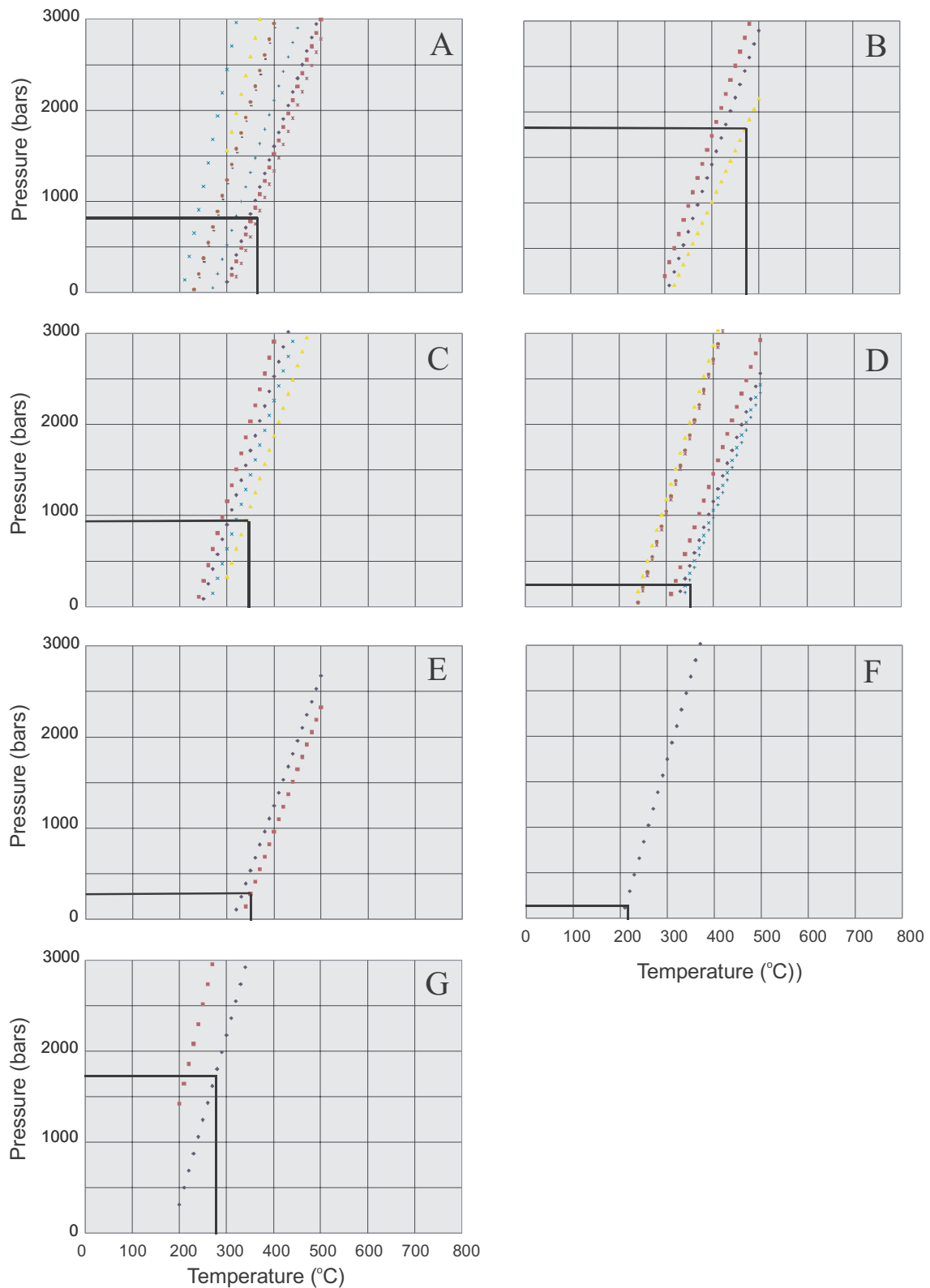


Figure 6. Isochore plots of minimum trapping conditions for type III B inclusions. (A) quartz phenocrysts, (B) quartz-tourmaline-chalcopyrite-pyrite vein in porphyry, (C) quartz-potassium feldspar-pyrite veins in the porphyry, (D) quartz-molybdenite-pyrite veins in the porphyry, (E) late quartz-pyrite vein, (F) quartz associated with massive sulphide in the mantos, (G) quartz associated with massive sulphide veins from Takla Silver Mine. Note the diagrams share common x and y axes. Lines defined by symbols are isochores; each line represents data from a single fluid inclusion assemblage. The fine, solid, vertical lines represent the final homogenization temperature (by halite dissolution) for the isochore that gives the minimum trapping condition for each diagram. The fine, solid, horizontal lines represent the corresponding pressure at the final halite dissolution temperature.

Trapping Conditions Based on Homogenization by Halite Dissolution

The relationship between halite dissolution temperatures and liquid-vapour homogenization temperatures for type III inclusions in quartz phenocrysts, veins and massive sulphide mineralization at Lustdust is illustrated in Figure 3. The diagonal line divides inclusions into type IIIA which exhibit final homogenization by vapour-bubble disappearance (lower right of Figure 3) and type IIIB which homogenize by halite dissolution (upper left of Figure 3).

Immiscible entrapment of dense type IIIB brines is precluded by phase-equilibria constraints. In the absence of evidence for fluid immiscibility, isochores of type IIIB inclusions provide better minimum trapping temperature estimates than other types of inclusions trapped in the one-phase field (Shepherd *et al.*, 1985). Disappearance of the vapour bubble in type IIIB inclusions at Lustdust generally occurs approximately 40 to 150°C lower than halite dissolution (Figure 3), which indicates moderate to high minimum trapping pressures.

Minimum trapping conditions for type IIIB inclusions in quartz phenocrysts, in veins in the porphyry, in massive sulphide mineralization from the mantos and in the No. 1 Zone vein are illustrated using isochore plots (Figure 6A to G). Minimum trapping pressures for each deposit and feature type are as follows: 880 bars (quartz phenocrysts, Figure 6A), 1.8 kb (quartz-tourmaline-chalcopyrite-pyrite veins, Figure 6B), 950 bars (quartz-potassium feldspar-pyrite veins, Figure 6C), 230 bars (quartz-molybdenite-pyrite veins, Figure 6D), 260 bars (late quartz + pyrite veins, Figure 6E), 170 bars (massive sulphide from mantos, Figure 6F), and 1.7 kb (No. 1 Zone vein, Figure 6G). Estimated depths of entrapment assuming lithostatic and hydrostatic loads are in Table 4.

Trapping Conditions Based on Critical Behaviour of Vapour-Rich Inclusions

Vapour-rich inclusions from the No. 1 Zone veins homogenize to both vapour (type II) and liquid (type IIQ) within an apparently narrow 20°C temperature range from 354 to 373°C. Type IIQ inclusions display unusual homogenization behaviour as the homogenized vapour bubble re-appears in virtually the same location as it disappears. True 'liquid-rich' inclusions typically show a period of a few degrees of cooling before the vapour bubble pops back in a different location (Cline and Vanko, 1995). The vapour bubble of type II inclusions from the outer veins does not appear to "grow" until it exhibits rapid expansion near the homogenization temperature. These types of behaviour indicate that these inclusions contain fluids with near-critical densities (Roedder, 1984; Cline and Vanko, 1995). Measured homogenization temperatures for vapour-rich inclusions may be significantly underestimated due to difficulties in observing disappearance of the liquid rim on the wall of the inclusion (Roedder, 1984; Bodnar *et al.*, 1985; Cline and Vanko, 1995).

Trapping conditions for type II fluids from the No. 1 Zone vein are indicated on a pressure-temperature projec-

tion of the H₂O-NaCl system for a 5 eq. wt. % NaCl fluid (Figure 7). The inclusions are interpreted to have been trapped during mild fluctuations in pressure (300 to 400 bars), temperature (400 to 440°C) and fluid composition (4 to 7.5 eq. wt. % NaCl) at near-critical conditions (see oval in Figure 7). The 'pressure correction' for type II fluid homogenization temperatures is approximately 45 to 70°C. At the maximum pressure of 400 bars and 440°C, rock is ductile, precluding open fractures except during short periods of high strain (Fournier, 1991; Hedenquist *et al.*, 1998). The No. 1 Zone vein is interpreted to have formed at depths between 1.1 and 1.5 km under lithostatic load (Table 4).

DISCUSSION AND SUMMARY

The Lustdust property is a polymetallic hydrothermal system in which mineralization is discontinuously developed over a 2.5 km strike length. The system is zoned, and includes Cu-Mo porphyry mineralization, carbonate replacement Cu-Au skarns and Zn mantos, and complex metallic (Zn-Pb-Ag-Au-As-Sb-Hg) massive sulphide-sulphosalt veins in limestones at the No. 1 Zone. Fluid inclusion studies at Lustdust were completed on the following types of minerals:

- (1) igneous quartz phenocrysts in the Glover Stock diorite and monzonite porphyry,
- (2) hydrothermal quartz in the various porphyry-style mineralized (Cu-Mo) and barren veins which cut the stock,
- (3) hydrothermal garnet and calcite crystals in the Cu-Au skarns,
- (4) late quartz in the Zn mantos, and
- (5) quartz and calcite in the quartz-sulphide-sulphosalt-bearing No. 1 Zone veins.

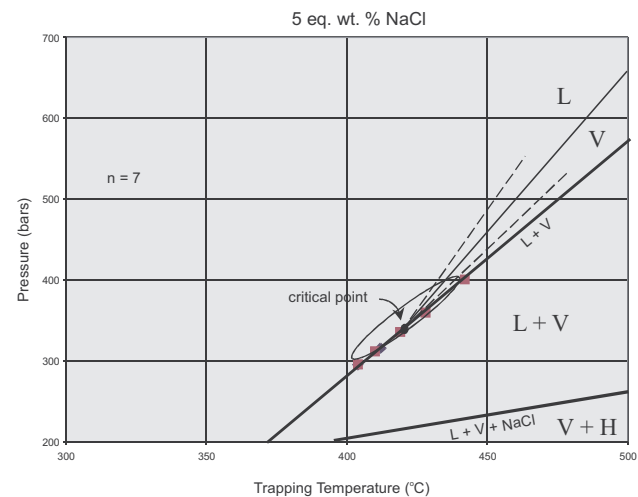


Figure 7. Pressure-temperature projection of the H₂O-NaCl system modified from Bodnar *et al.* (1985). The dark line (L + V) represents the liquid-vapour curve for a 5 eq. wt. % NaCl fluid similar to the composition of type II inclusions in samples GR01-104 and GR01-105 from the Takla Silver Mine No. 1 Zone veins. The critical point for this fluid is indicated. The oval indicates trapping conditions for type II inclusions, which homogenize to the liquid and vapour phases at near-critical conditions.

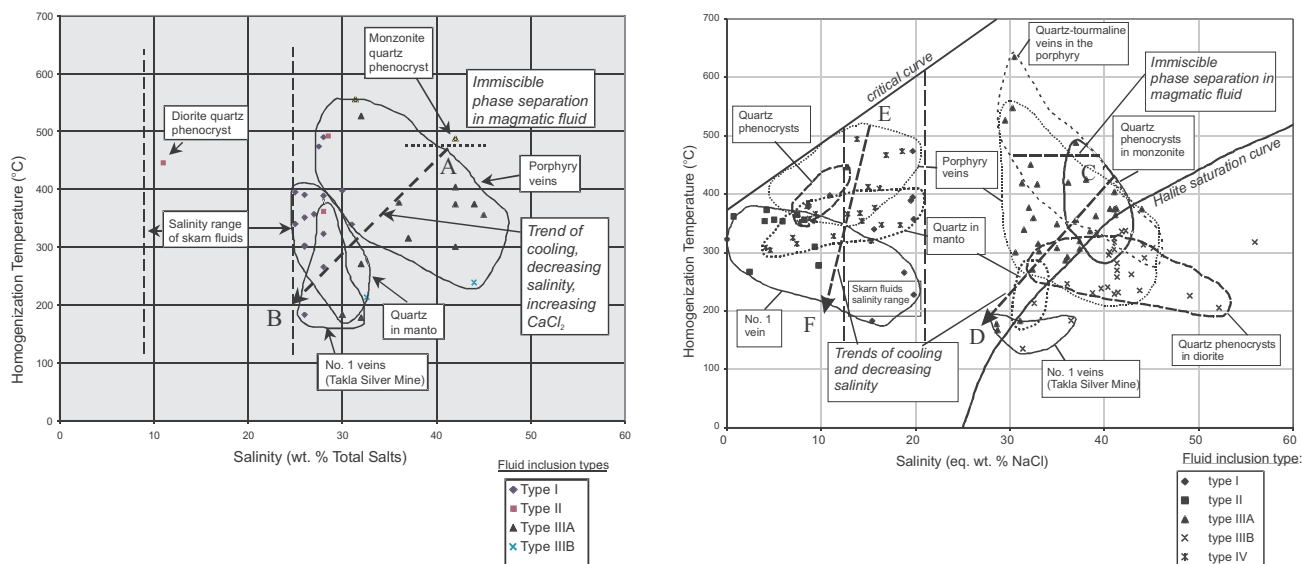


Figure 8. Homogenization temperature - salinity relationships in fluid inclusions from the Lustdust property (format from Lang and Baker, 1999). (a) Salinity is in weight percent total salts calculated from the H_2O - $NaCl$ - $CaCl_2$ ternary diagram in Figure 4. (b) Salinity is in equivalent weight percent $NaCl$ calculated using the equations of Bodnar and Vityk (1994) and freezing point depression data. Note that range of salinity of skarn fluids is indicated by broad dashes. Trends of decreasing temperature and salinity are represented by thick, dark dashed lines with arrows (lines A-B, C-D and E-F).

The studies place constraints on the fluid evolution of the Lustdust hydrothermal system. Each style of mineralization has unique fluid inclusion populations and compositions indicating they were trapped under specific conditions that change spatially and temporally.

Fluid inclusions in the monzonite quartz phenocrysts and the Cu-Mo-bearing porphyry veins comprise coexisting high salinity H_2O - $NaCl$ - $CaCl_2$ $MgCl_2 \pm FeCl_2$ (Type III) and vapour-rich H_2O - CO_2 - $NaCl$ - CH_4 (Type IV) fluids. These fluids were trapped as immiscible phases at maximum homogenization temperatures of approximately 475 to 500°C (see horizontal dotted line in Figures 8a and 8b). For comparison, salinities are calculated as weight percent total salts (35 to 45 weight percent at maximum homogenization temperatures) in Figure 8a and as equivalent weight percent $NaCl$ (30 to 40 equivalent weight percent at maximum homogenization temperatures) in Figure 8b. Fluids, in both diagrams, plot along trends of decreasing temperature and salinity (Path A-B, Figure 8a and Path C-D, Figure 8b) and increasing $CaCl_2$ concentration (cf. Figure 4). A second cooling trend, for immiscible Type II or IV and I fluids, at maximum homogenization temperatures of 450 to 500°C and salinities of 12 to 20 equivalent weight percent $NaCl$ is inferred in Figure 8b (Path E-F). Similar temperature-salinity relationships have been reported in high-temperature, carbonate-hosted Zn-Pb-AgCu skarn-manto deposits in Mexico (Lang and Baker, 1999).

At Lustdust, pressure estimates, assuming immiscible entrapment in a lithostatic pressure regime and considering the presence of CO_2 , indicate deposition of late magmatic fluids at the following depths (Table 4):

- Monzonite quartz phenocrysts: 1.9 km
- Porphyry veins: 1.7 to 1.9 km

Mantos: 1.2 km

The No. 1 Zone veins are interpreted to have formed under near critical conditions in a lithostatic pressure regime at depths between about 1.1 to 1.5 km.

Depth estimates at Lustdust, assuming immiscible entrapment in an open system (hydrostatic pressure regime), range from about 3.0 to 5.0 km (Table 4).

Field evidence, including the lack of ductile structures, abundance of brittle faulting and the development of the extensive skarn envelope, suggests the Lustdust mineralization formed at relatively shallow depths (Ray *et al.*, 2002, this volume). Consequently, the minimum estimated trapping pressures for some type IIIB inclusions that homogenize by halite dissolution seem unreasonably high (see Table 4: quartz-tourmaline-chalcopyrite-pyrite veins and the No. 1 Zone veins). The discrepancy between geologic and other fluid inclusion evidence, trapping pressure estimates based on observed fluid immiscibility, and the estimates based on halite dissolution may be explained if the composition of the fluids (H_2O - $NaCl$ - $CaCl_2 \pm MgCl_2 \pm FeCl_2$) is considered. Stewart and Potter (1979) show that the introduction of Ca^{2+} ion reduces the slopes of isochores calculated using $NaCl$ - H_2O model composition. Reduced isochore slopes would result in lower calculated pressure estimates for the type IIIB inclusions.

At Lustdust, the temporal and spatial occurrence of early type III (liquid-rich, high salinity) inclusions coexisting with types IV and II (vapour-rich inclusions) followed by later type I (liquid-rich, low salinity) inclusions is characteristic of the productive portions of shallow magmatic-hydrothermal systems associated with porphyry Cu deposits (Beane and Bodnar, 1995). Although CO_2 is not typical in most porphyry Cu deposits, it is more common in

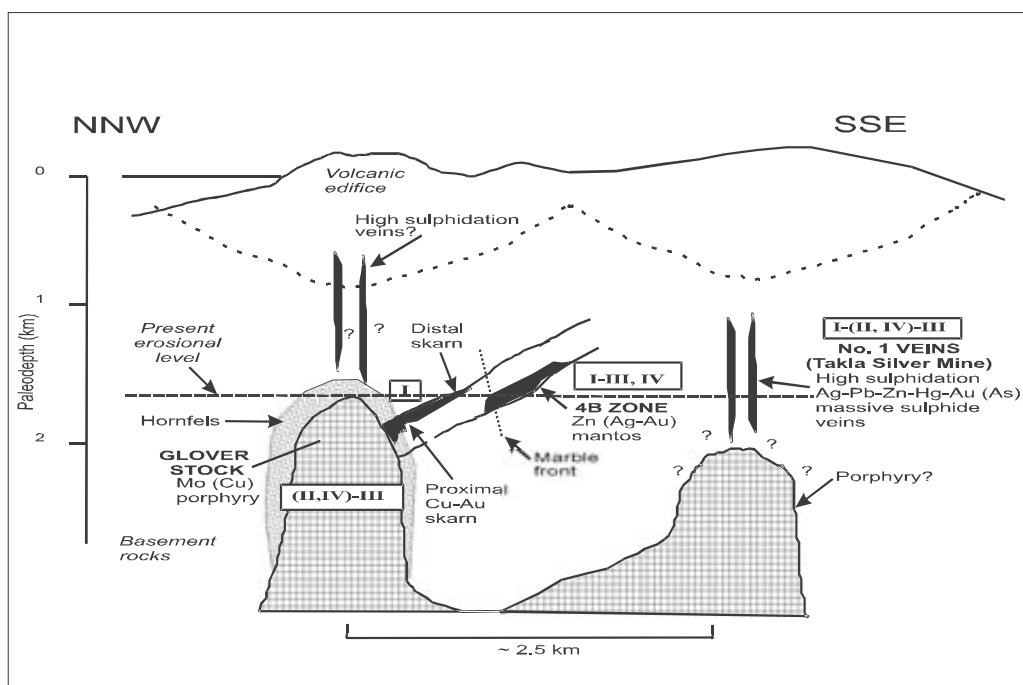


Figure 9. NNW-SSE section showing idealized lateral and vertical zoning of deposit types and principal metals at the Lustdust prospect, adapted from a general exploration model by Sillitoe (1995). Depths are calculated assuming a lithostatic pressure regime. The composition of fluids that characterize different portions of each type of system are indicated: I = low-moderate salinity, liquid dominated; II = low salinity, vapour dominated; III = high salinity, liquid dominated; IV = low salinity, vapour dominated, CO₂ bearing (concept after Lang *et al.*, 2000).

porphyry-Mo systems (Beane and Bodnar, 1995; Roedder, op. cit.). CO₂ in vapour-rich inclusions is reported at Santa Rita, New Mexico (Reynolds and Beane, 1985) and is recognized in other deposits such as Bingham, Utah, El Salvador, Chile, and Sar Cheshmeh, Iran (Roedder, 1984).

The Lustdust prospect represents a classic magmatic-related and zoned system similar to those described by Sillitoe (1995), Megaw (1998) and Lang *et al.* (2000). The fluid zoning at Lustdust is characterized as follows (Figure 9):

Porphyry: Hydrothermal fluid types IV and II (vapour-rich ± CO₂-bearing) and type III (liquid-rich, high salinity, halite-bearing)

Skarn: Hydrothermal fluid type I (liquid-rich, low salinity)

Manto: Hydrothermal fluid types I and III (liquid-rich, low and high salinity) and type IV (vapour-rich, CO₂-bearing).

No.1 Zone Veins: Hydrothermal fluid types I and III (liquid-rich, low and high salinity) and types II and IV (vapour-rich ± CO₂-bearing)

The No. 1 Zone veins give estimated depths of 1.1 to 1.5 km, assuming trapping at near-critical conditions. The occurrence of abundant vapour-rich inclusions (Types II and IV) in quartz from the veins suggests that they formed above a magmatic intrusion. The presence of type III (salt-saturated) inclusions, together with the occurrence of sulphosalts and significant arsenopyrite (~7 to 15 %, Leitch, 2001) in dominantly massive sulphide veins suggests that

these veins may have formed in a high sulphidation environment above a porphyry, similar to those described by Sillitoe (1995) and Lang *et al.* (2000). Thus, the No. 1 Zone veins may overlie a southern extension of the Glover Stock or be related to a separate buried intrusion (Figure 9). This possibility and the Hg-rich nature of the veins is significant for regional exploration because the presence elsewhere of Hg occurrences and/or Takla Silver-type veins may indicate the existence of a Lustdust-type target.

ACKNOWLEDGMENTS

We are grateful to the management and staff of Alpha Gold Corp for their assistance during this project, particularly George Whatley (President, Alpha Gold). Thanks to M.J. Orchard of the Geological Survey of Canada for identifying conodont microfossils. Many of the geological ideas expressed in this paper were derived from discussions in the office and field with Peter Megaw (President, IMDEX), Jim McGlassen, Ian Webster, the late Keith Glover, and Craig Leitch. Editing by Brian Grant and Ian Webster are also appreciated.

REFERENCES

- Beane, R.E. and Bodnar, R.J. (1995): Hydrothermal Fluids and Hydrothermal Alteration in Porphyry Copper Deposits; *in* Porphyry Copper Deposits of the American Cordillera, F.W. Pierce and J.G. Bolm, Editors, *Arizona Geological Society*, Digest 20, pages 83-93.
- Bodnar, (1995): Fluid-Inclusion Evidence for a Magmatic Source for Metals in Porphyry Copper Deposits; *in* Magmas, Fluids,

- and Ore Deposits, J.F.H. Thompson, Editor, *Mineralogical Association of Canada*, Short Course, Volume 23, pages 139-152.
- Bodnar, R.J. and Vityk, M.O. (1994): Interpretation of Microthermometric Data for H₂O-NaCl Fluid Inclusions; in *Fluid Inclusions in Minerals: Methods and Applications*, Short Course of the Working Group (IMA) "Inclusions in Minerals", B. De Vivo and M.L. Frezzotti, Editors, *Virginia Polytechnic Institute and State University*, pages 117-130.
- Bodnar, R.J., Burnham, C.W. and Sterner, S.M. (1985): Synthetic Fluid Inclusions in Natural Quartz. III. Determination of Phase Equilibrium Properties in the System H₂O-NaCl to 1000°C and 1500 bars; *Geochimica et Cosmochimica Acta.*, Volume 49, pages 1861-1873.
- Bowers, T.S. and Helgeson, H.C. (1983): Calculation of the Thermodynamic and Geochemical Consequences of Nonideal Mixing in the System H₂O-CO₂-NaCl on Phase Relations in Geologic Systems: Equation of State for H₂O-CO₂-NaCl Fluids at High Pressures and Temperatures; *Geochimica et Cosmochimica Acta.*, Volume 47, pages 1247-1275.
- Brown, P.E. and Hagemann, S.G. (1994): MacFlincor: A Computer Program for Fluid Inclusion Data Reduction and Manipulation; in *Fluid Inclusions in Minerals: Methods and Applications*, Short Course of the Working Group (IMA) "Inclusions in Minerals", B. De Vivo and M.L. Frezzotti, Editors, *Virginia Polytechnic Institute and State University*, pages 231-250.
- Cline, J.S. and Vanko, D.A. (1995): Magmatically Generated Saline Brines Related to Molybdenum at Questa, New Mexico, USA; in *Magmas, Fluids, and Ore Deposits*, J.F.H. Thompson, Editor, *Mineralogical Association of Canada*, Short Course, Volume 23, pages 153-174.
- Crawford, M.L. (1981): Phase Equilibria in Aqueous Fluid Inclusions; in *Fluid Inclusions: Applications to Petrology*, L.S. Hollister and M.L. Crawford, Editors, *Mineralogical Association of Canada*, Short Course Handbook 6, pages 75-100.
- Evans, G. (1996): Geological and Geochemical Report on the 1996 Exploration of the Lustdust Property; submitted by Teck Corp., *British Columbia Ministry of Energy and Mines*, Assessment Report 24735, 125 pages.
- Evans, G. (1998): Diamond Drilling Report on the 1998 Exploration of the Lustdust Property; submitted by Alpha Gold, *British Columbia Ministry of Energy and Mines*, Assessment Report 25739, 77 pages.
- Fournier, R.O. (1991): Transition from Hydrostatic to Greater Than Hydrostatic Fluid Pressures in Presently Active Hydrothermal Systems in Crystalline Rocks; *Geophysical Research Letters*, Volume 18, pages 955-958.
- Gabrielse, H., and Yorath, C.J. (1992): Geology of the Cordilleran Orogeny in Canada. *Geological Society of America*, DNAG G-2, 875 pages.
- Goldstein, R.H. and Reynolds, T.J. (1994): Systematics of Fluid Inclusions in Diagenetic Minerals; *Society for Sedimentary Geology*, Short Course 31, 199 pages.
- Hedenquist, J.W., Arribas, A. Jr. and Reynolds, T.J. (1998): Evolution of an Intrusion-Centered Hydrothermal System: Far Southeast-Lepanto Porphyry and Epithermal Cu-Au Deposits, Philippines; *Economic Geology*, Volume 93, No. 4, pages 373-404.
- Jacobs, G.K. and Kerrick, D.M. (1981): Methane: An Equation of State with Application to the Ternary System H₂O-CO₂-CH₄; *Geochimica et Cosmochimica Acta*, Volume 45, pages 607-614.
- Lang, J.R. and Baker, T. (1999): The Role of Fluid Immiscibility in Some Mexican Skarn Deposits; in *Mineral Deposits: Processes to Processing*, C.J. Stanley et al. Editors, *Balkema Publishing*, Rotterdam, pages 1047-1050.
- Lang, J.R., Baker, T., Hart, J.R. and Mortensen, J.K. (2000): An Exploration Model for Intrusion-Related Gold Systems; *Society of Economic Geologists*, Newsletter, No. 40, pages 1 to 15.
- Leitch, C.H.B. (2001): Petrographic Report on Polished Thin Sections of 7 Samples; *British Columbia Geological Survey*, Internal Report.
- Linke, W.F. (1958): Solubilities of Inorganic and Metal Organic Compounds, Volume I.; *D. Van Nostrand Col*, Princeton, New Jersey; 1487 pages.
- Linke, W.F. (1965): Solubilities of Inorganic and Metal Organic Compounds, Volume II; *American Chemical Society*, Washington, D.C.; 1914 pages.
- Megaw, P.K.M. (1998): Carbonate-hosted Pb-Zn-Ag-Cu-Au replacement deposits: An Exploration Perspective; in *Mineralized Intrusion-Related Skarn Systems*, D.R. Lentz, Editor, *Mineralogical Association of Canada*, Short Course Series, Volume 26, pages 337-358.
- Megaw, P.K.M. (1999): Report on 1999 drilling and geological study of the Lustdust property, Omineca Mining Division, British Columbia; submitted by *Alpha Gold Corporation*, October 1999, *British Columbia Ministry of Energy and Mines*, Assessment Report 26069, 151 pages.
- Megaw, P.K.M. (2000): Report on 2000 drilling and geological study of Lustdust property, Omineca Mining Division, British Columbia; submitted by *Alpha Gold Corporation*, October 2000, *British Columbia Ministry of Energy and Mines*, Assessment Report 26466, 396 pages.
- Megaw, P.K.M. (2001): Report on 2001 drilling and geological study of Lustdust property, Omineca Mining Division, British Columbia; submitted by *Alpha Gold Corporation*, October 2001, *British Columbia Ministry of Energy and Mines*, Assessment Report, 40 pages.
- Monger, J.W.H. (1977): Upper Paleozoic rocks of the western Canadian Cordillera and their bearing on Cordillera evolution. *Canadian Journal of Earth Science*, volume 14, p. 1832-1859.
- Monger, J.W.H. (1998): Plate tectonics and northern Cordilleran geology: An unfinished revolution. *Geoscience Canada*, volume 24:4, p. 189-198.
- Oakes, C.S., Bodnar, R.J. and Simonson, J.M. (1990): The System NaCl-CaCl₂-H₂O: I. The Ice Liquidus at 1 Atm Total Pressure; *Geochimica et Cosmochimica Acta*, Volume 54, pages 603-610.
- Paterson, I.A. (1974): Geology of Cache Creek Group and Mesozoic rocks at the northern end of the Stuart Lake Belt, central British Columbia; Report of Activities, *Geological Survey of Canada*, Paper 74-1, Part B, p. 31-42.
- Paterson, I.A. (1977): The geology and evolution of the Pinchi Fault Zone at Pinchi Lake, central British Columbia; *Canadian Journal of Earth Science*, volume 14, p. 1324-1342.
- Potter, II, R.W. and Clyne, M.A. (1978): Solubility of Highly Soluble Salts in Aqueous Media - Part 1., NaCl, KCl, CaCl₂, Na₂SO₄, and K₂SO₄ Solubilities to 100°C; *United States Geological Survey*, Journal of Research, Volume 6, pages 701-705.
- Ray, G.E., Webster, I.C.L., Megaw, P.K.M., McGlasson, J., and Glover, J.K. (2002, this volume): The Lustdust property in central British Columbia: A polymetallic zoned porphyry-skarn-manto-vein system; *British Columbia Ministry of Energy and Mines*, Geological Fieldwork 2001, Paper 2001-1.
- Reynolds, T.J. and Beane, R.E. (1985): Evolution of Hydrothermal Fluid Characteristics at the Santa Rita, New Mexico, Porphyry Copper Deposit; *Economic Geology*, Volume 80, No. 5, pages 1328-1347.
- Roedder, E. (1984): Fluid Inclusions; *Mineralogical Society of America*, Reviews in Mineralogy, Volume 12, 644 pages.
- Schiarizza, P. (2000): Bedrock geology, Old Hogem (Western Part), NTS 93N/11, 12, 13, 1:100 000 scale compilation

- map, *British Columbia Ministry of Energy and Mines*, Open File 2000-33.
- Schiarizza, P., and MacIntyre, D. (1999): Geology of the Babine Lake-Takla Lake area, central British Columbia (93K/11, 12, 13, 14: 093N/3, 4, 5, 6). *B.C. Ministry of Energy, Mines and Petroleum Resources*, Geological Fieldwork 1998, Paper 1999-1, pages 33-68.
- Shepherd, T.J., Rankin, A.H. and Alderton, D.H.M. (1985): A practical Guide to Fluid Inclusion Studies; *Blackie & Son Ltd.*, London, 239 pages.
- Sillitoe, R.H. (1995): The Influence of Magmatic-Hydrothermal Models on Exploration Strategies for Volcano-Plutonic Arcs; in *Magmas, Fluids, and Ore Deposits*, J.F.H. Thompson, Editor, *Mineralogical Association of Canada*, Short Course, Volume 23, pages 511-525.
- Stewart, D.B. and Potter, II, R.W. (1979): Application of Physical Chemistry of Fluids in Rock Salt at Elevated Temperature and Pressure to Repositories for Radioactive Waste; in *Scientific Basis for Nuclear Waste Management*, G.J. McCarthy, editor, *Wiley Interscience*, New York, pages 236-277.
- Vanko, D.A., Bodnar, R.J. and Sterner, S.M. (1988): Synthetic Fluid Inclusions: VIII. Vapour-Saturated Halite Solubility in Part of the System NaCl-CaCl₂-H₂O, with Application to Fluid Inclusions from Oceanic Hydrothermal Systems; *Geochimica et Cosmochimica Acta.*, Volume 52, pages 2451-2456.
- Wheeler, J.O., Brookfield, A.J., Gabrielse, H., Monger, J.W.H., Tipper, H.W. and Woodsworth, G.J. (1991): Terrane map of the Canadian Cordillera; *Geological Survey of Canada*, Map 1713a, Scale 1:2 000 000.